uOttawa

L'Université canadienne
Canada's university

Gas Separation by Adsorption In Order to Increase CO_2 Conversion to CO Via Reverse Water Gas Shift (RWGS) Reaction

By
Farhang Abdollahi
Master of Applied Science Thesis

Submitted to the School of Graduate Studies and Research
in partial fulfillment of requirements
for degree of M.A.Sc in Environmental Engineering

Supervisors:
Dr. Handan Tezel

Ottawa-Carleton Institute for Environmental Engineering
Department of Civil Engineering
University of Ottawa
Ottawa, Canada

Abstract

In this research project, adsorption is considered in conjunction with the reverse water gas shift reaction in order to convert CO_2 to CO for synthetic fuel production. If the CO_2 for this process can be captured from high emitting industries it can be a very good alternative for reduced fossil fuel consumption and GHG emission mitigation. CO as an active gas could be used in Fischer-Tropsch process to produce conventional fuels. Literature review and process simulation were carried out in order to determine the best operating conditions for reverse water gas shift (RWGS) reaction. Increasing CO_2 conversion to CO requires CO_2/CO separation downstream of the reactor and recycling unreacted CO_2 and H_2 back into the reactor. Adsorption as a viable and cost effective process for gas separation was chosen for the CO_2/CO separation. This was started by a series of adsorbent screening experiments to select the best adsorbent for the application. Screening study was performed by comparing pure gas isotherms for CO_2 and CO at different temperatures and pressures. Then experimental isotherm data were modeled by the Temperature-Dependent Toth isotherm model which provided satisfactory fits for these isotherms. Henry law's constant, isosteric heat of adsorption and binary mixture prediction were determined as well as selectivity for each adsorbent. Finally, the expected working capacity was calculated in order to find the best candidate in terms of adsorption and desorption. Zeolite NaY was selected as the best candidate for CO_2/CO separation in adsorption process for this project. In the last step breakthrough experiments were performed to evaluate operating condition and adsorption capacity for real multi component mixture of CO_2, CO, H_2 in both cases of saturated with water and dry gas basis. In multi components experiments zeolite NaY has shown very good performance to separate CO_2/CO at low adsorption pressure and ambient temperature. Also desorption experiment was carried out in order to evaluate the working capacity of the adsorbent for using in industrial scale and eventually temperature swing adsorption (TSA) process worked very well for the regeneration step. Integrated adsorption system downstream of RWGS reactor can enhance the conversion of CO_2 to CO in this process significantly resulting to provide synthetic gas for synthetic fuel production as well as GHG emission mitigation.

Acknowledgements:

I would like to first thank my supervisor Dr. F. Handan Tezel for providing me this opportunity and all her supports to accomplish this thesis. Thanks to her help and trust I was able to work enthusiastically on this project and grateful for her patience I have overcome unexpected difficulties in the research road.

Many thanks to Phoenix Canada oil Co Ltd for sponsoring this project and their representative Mr. Stephen Aplin (HDP group, environment and energy director). Mr. Aplin's advices and guidance on energy section helped me a lot in order to lead the project forward.

Also I would like to thank all members of the SMART group and my co-workers, Dean Kennedy, Patrick Charlebois, Qian Yang, Niloofar Abdehagh, Muhammad Tawalbeh, Abubak Waraith, Burcu Ugur for their work, help and advice they gave me during my studies.

Here I would like to give special thanks to support stuff and technicians in Chemical and Biomedical Engineering Department namely Mr. Louis Tremblay, Mr. Franco Ziroldo, Mr. Gerard Nina who helped me and trained me in the equipment preparation, lab set-up and programing.

Finally I would like to thank my family, parents and especially my wife for her patience and encouragement entire of my graduate studies; I could have not completed this degree it without their supports.

Statement of Contributions of Collaborators:

Hereby I declare that I am the first and main author of this thesis which was completed under supervision of Dr. F. H. Tezel. The Lab-scale adsorption set-up was designed, procured and prepared with some helps from the technical stuff, Louis Tremblay, Gerard Nina and Franco Ziroldo. I have repaired and adjusted the gas chromatograph by guidance of Louis Tremblay and Gerard Nina helped me set up data acquisition system for the experiments. I performed all of the experiments for breakthrough tests; as well as all gravimetric system pure gas isotherms. However, some of the pure gas isotherms on volumetric system were performed by Abubakr Waraith, Patrick Charlebois and Qian Yang after that they were trained by the candidate. I have carried out RWGS process design and simulation by UNISM (HYSYS) under Dr. Tezel supervision.

Table of Contents

List of Figures

List of Tables

Nomenclature

ΔH	Heat of adsorption	(kJ/mol)
ΔP	Pressure drop across the bed	(atm)
A	Length	angstrom
Å^{3}	Atomic volume	Å$^{3} = 10^{-24}$ Cm3
b	Langmuir and Toth isotherm parameter for adsorption affinity	(atm^{-1})
b_0	Affinity Parameter at the Reference Temperature	(atm^{-1})
C^p	Concentration in the particle	(mol/m^{3})
C_g	Concentration in the bulk phase	(mol/m^{3})
C_i	Inlet mole fraction of the component i	dimensionless
C_{i0}	Outlet mole fraction of the component i	dimensionless
C_{inlet}	Concentration in the inlet	(mol/m^{3})
D_e	Molecular diffusivity	(m/s)
D_p	Equivalent spherical diameter of the packing	dimensionless
D	Debye	1 D = 10^{-18} statC·cm
DQ	Deviation of experimental amounts	dimensionless
EWC	Expected working capacity	(mmol/g)
K_0	Henry’s Law constant	(mmol/g/atm)
K_f	Mass transfer coefficient	(m/s)
k_y	Rate constant	(ml/min/g)
L	Length of the bed	(m)
m	Mass of the adsorbent	(g)
P	Pressure	(atm)
q	Amount of adsorbed gas	(mmol/g)
q_{exp}	Experimental amount of adsorbed gas	(mmol/g)
q_{cal}	Calculated amount of adsorbed gas	(mmol/g)
Q	Volume flow rate in the adsorption column	(ml/min)
Q_{iso}	Isosteric heat of adsorption	(kJ/mol)
q_s	Maximum amount of adsorbed gas	(mmol/g)
q_{s0}	Maximum Amount Adsorbed at the Reference Temperature	(mmol/g)
q_m	Maximum capacity of the adsorbent	(mg $_{gas}$/g $_{ads}$)
R	Gases constant	(kJ/mol/K)
R_p	Particle radius	(cm)
$S_{i/j}$	Selectivity	dimensionless
T	Temperature	(K)
Z	Length of saturated bed	(cm)
t	Toth isotherm parameter	dimensionless
t	Adsorption time	(second)
T_0	Reference Temperature	(K)
t_0	Toth Isotherm Parameter at the Reference Temperature	dimensionless
t_i	Area above breakthrough curve	(min)
V	Volume of the column	(m^{3})

ρ	Density of fluid	(Kg/m^3)
μ	Dynamic viscosity of the fluid	(Cp)
Φ	Sphericity	dimensionless
α	Toth Isotherm Parameter	dimensionless
χ	Toth Isotherm Parameter	dimensionless
ε_c	Void fraction of the column	dimensionless
ν_g	Superficial velocity	(m/s)

Chapter I: Introduction

1. Introduction

Large amounts of carbon dioxide (CO_2) will be available in a near future when carbon capture and sequestration (CCS) begins to be implemented in Canadian power generation. Many industries including coal power plants will have to sequester CO_2 and manage the concentrated stream to avoid penalties for their emission. This captured CO_2 should be used in an efficient and productive way rather than being stored underground or sequestered at the bottom of the oceans. There are currently 234 active or planned carbon capture projects around the world, 77 of them are large scale project to test CCS value (Chemistry world, 2011). If the captured CO_2 is used as feedstock for other processes the cost of CO_2 can be a zero cost (or even with negative value). The power plants and industries emit the same amount of CO_2 as transportation system from petroleum based fuel in Canada (Environment Canada, 2010). The CO_2 emitted by industries which are mainly power plants, could be captured by using proven methods such as absorption, adsorption or membrane separations. This raises the potential of enormous amounts of CO_2 becoming available as a raw material for the CO component of synthetic fuel. Recycling CO_2 in a proper way presents the prospect of revenue for the companies who capture it (versus a cost if they sequester it), and thereby may make CCS an economically viable way of reducing CO_2 emissions. CO_2 can be split into carbon monoxide (CO, a valuable precursor to numerous chemical products) by reacting it with hydrogen (H_2). If H_2 is manufactured by splitting water using low- or zero-carbon energy (like excess heat in nuclear power plant), then synthetic gas (CO and H_2) may be manufactured from captured CO_2 and water-derived H_2 as a precursor for “low carbon” products, and many products could be manufactured from it. Furthermore due to excess energy in some sources such as nuclear power plant or wind and solar sources especially at the off-peak periods, an appropriate combination of processes could make it feasible to have an alternative energy to cover all of the energy needed for the transportation sector. It must be noted that conventional fuel such as gasoline and diesel still are the best and the most valuable energy for transport section while hydrogen derived vehicles and fuel cells could have a long way to reach the viable application in the world. Energy storage in liquid fuel could be many times greater than for example Li-ion batteries or other sources of energy. Conventional processes such as the Fischer-Tropsch and methanol production processes, low carbon liquid fuel could be manufactured by synthetic gas. These processes can reduce the petroleum-based fuel and CO_2 emission by half. In the other hand, by launching the synthetic fuel plants in different regions, close to power plants, majority of petroleum based fuel transportation costs could be compensated. By converting CO_2 to CO we could provide syngas for synthetic fuel production which could be the most viable approach to reduce GHG impact and reduce petroleum consumption in Canada. Therefore by studying all possibilities to increase the CO_2 to CO conversion via one of the known reaction named Reverse Water Gas Shift reaction (RWGS), we could introduce an excellent alternative way for CO_2 management.

2. RWGS reaction

In the Reverse Water Gas Shift reaction (RWGS) CO_2 reacts with H_2 to produce CO and water. RWGS reaction is based on following endothermic reaction:

$$CO_2 + H_2 = CO + H_2O \qquad \Delta H = +41.12 \text{ kJ/gmol (endothermic)} \tag{1}$$

Then the CO product could be reacted with H_2 in the Fischer-Tropsch reaction or methanol formation reactions to produce low carbon liquid conventional fuels based on following reactions:

$$(2n + 1)\, H_2 + n\, CO \rightarrow C_nH_{(2n+2)} + n\, H_2O \tag{2}$$

$$CO + 2\, H_2 \rightarrow CH_3OH \tag{3}$$

Demand of energy for transportation is increasing and the consumption of fossil fuel is the major concern in transport section. Table 1 shows comparison of synthetic fuel from CO_2 and H_2 with other sources of energy used in the transport section. As shown in this table the net CO_2 released for the fuel derived from CO_2/H_2 is zero due to conversion of CO_2 to fuel. At the same time water or wind power as renewable resources can be used to produce H_2 instead of non-renewable natural resources such as fossil fuels, methane, etc.

Table 1 Fuel needed and CO_2 released for alternate transportation fuel sources, (Schultz et al., 2009).

Units: MMt/yr	Transportation Fuel Form			
	Oil	**Coal**	**Coal + H_2 from water**	**CO_2+H_2 from water**
Oil needed	612	--	--	--
Coal needed	--	1113	556	0
H_2 needed	--	--	130	260
CO_2 needed	~100	2046	104	-1811
CO_2 released on use	1811	1811	1811	1811
Net CO_2 released	1911	3857	1905	0
Current total CO_2 production 5682 MMt/yr				
Current C as coal use/CO_2 produced 565/2070 MMt/yr. H_2 use: 10 MMt/yr				

This process is economically competitive with conventional processes with respect to factors mentioned before, providing the following conditions are met:

- Minimize as much as possible the consumption of hydrogen,
- Produce fuels that can be easily stored and transported, and
- Use low-carbon energy sources.

In this study RWGS reaction will be compared briefly with the other CO_2 conversion processes to ensure that it is the best option for CO production such as dry reforming of methane, direct hydrogenation of CO_2 and the Sabatier reaction. Then all factors affecting RWGS reaction will be discussed.

In order to achieve the highest feasible conversion of CO_2 for the overall process, separation and recycling of unreacted CO_2 and H_2, or removing of CO and H_2O are considered subsequently. Since RWGS reaction is an equilibrium reaction, one of the proposed methods for increasing overall conversion in the literature is removing the water from the outlet stream by condensing, then heating the stream again and sending it into the next RWGS reactor and repeat this process for removing as much water as possible to drive reaction toward products side (Doty et al, 2010). A drawback of this method is the energy consumption for cooling and heating stream by means of very high efficiency heat exchangers and also conversion would not be high enough to convert most of CO_2 in the system. A potential remedy could be a separation system after the RWGS reactor in order to recycle back unreacted CO_2 to the inlet of RWGS reactor.

There are various methods for capturing CO_2 from effluent streams by membrane separation, pressure swing adsorption, amine absorption and cryogenic methods. CO_2 separation by membrane has been investigated in steam methane reforming industries. Membrane can be very useful in the future if their performance is improved. Currently it is very hard to trust them for long term applications in industrial scale due to many reasons such as stabilities, toxicities of the components after a long time for high volume operations. One of the most feasible and reliable industrial gas separation processes is adsorption. Separation of CO_2 from stream including CO needs to be investigated more, since their molecular sizes are closer than other components such as water and hydrogen which have smaller molecular size. Therefore, an adsorbent screening was started to find a suitable adsorbent to separate CO_2 from CO in the stream including CO_2, CO, H_2 and water. So pure gas isotherms for CO_2 and CO have been carried out and interpreted for different commercial adsorbents. The results were modeled and predicted for choosing the best adsorbent for these gases since there are not sufficient studies done specifically on CO_2/CO separation by adsorption. Subsequently selected adsorbent has been tested and studied in a prepared set up in the adsorption lab of University of Ottawa to ensure the feasibility and efficiency of the separation system in the case of real multi-component mixture.

3. General objective of this study:

The goal of this project is therefore to develop a method for economic conversion of CO_2 into CO via RWGS reaction. A preliminary project (Engage # EGP 402456-10) developed a feasible, un-optimized flow sheet for an RWGS reactor. The currently proposed project would build on that flow sheet (the “base-case design”) to develop an optimized process design that includes the ease of product recovery, un-reacted CO_2 recycling in process for increasing conversion of CO_2 to CO.

4. Thesis structure:

The current thesis structure is a paper-based thesis. The first chapter describes the importance of the work and presents general introduction as well as researches objective to be undertaken. Chapter II-IV are scientific papers which either were submitted and accepted or are being submitted to appropriate referred journals. Chapter II presents simulation and process design of RWGS reaction in order to convert CO_2 to CO and provide syngas for low carbon liquid fuel production. Simulation has been performed by means of UNISIM software in this chapter and a novel process for RWGS has been determined. Chapter III presents an experimental adsorbent screening study for CO_2/CO separation downstream of RWGS reactor. In this chapter different adsorbents selected by literature review for gas separation were tested to choose the best candidate for further studies in following chapters. Adsorption equilibrium isotherm for the pure gases and modeling were applied and results fitted with experimental data. Then based on experimental data and modeling parameters prediction of multi component adsorption was carried out. Eventually the most suitable adsorbents were chosen in order to be tested in real condition with multi component feed gas in an adsorption column. In chapter IV breakthrough experiments for different gas compositions and operation conditions were conducted and experimental results have been modeled in order to determine necessary information for adsorption separation design. Finally Chapter V looks to the general conclusions drawn from each paper and works done in this research. Also the final chapter includes some recommendations and potential investigation for future works in order to further develop the concepts proposed in this thesis for industrial scale applications.

5. References:

Doty, F. D., G. N. Doty, J. P. Staab and L. L. Holte (2010). "Toward efficient reduction of CO_2 to CO for renewable fuels." Es2010: Proceedings of ASME 4th International Conference on Energy Sustainability, Vol 1: 775-784.

Schultz, K., S. L. Bogart, R. P. Noceti and A. V. Cugini (2009). "Synthesis of hydrocarbon fuels using renewable and nuclear energy." Nuclear Technology 166(1): 56-63.

http://www.rsc.org/chemistryworld/Issues/2011/April/BusinessRoundup.asp

http://www.ec.gc.ca/indicateurs-indicators/default.asp?lang=en&n=54C061B5-1

Chapter II: Increasing Conversion of CO_2 to CO via RWGS Reaction: Simulation and Process Design

Farhang Abdollahi(1), F. Handan Tezel(1), Stephen Aplin(2)

(1) University of Ottawa, Department of Chemical and Biological Engineering, Ottawa, ON, Canada

(2) The HDP Group, Ottawa, ON, Canada

Keywords: Alternative energy, CO_2 conversion, Synthetic fuel, Reverse water gas shift reaction (RWGS)

Abstract

While most carbon capture and sequestration (CCS) proposals envision permanent underground storage for captured CO_2, increasing attention is being paid to ways in which captured CO_2 could be utilized as a raw material for the manufacture of subsequent chemicals. One such proposal is reacting CO_2 with hydrogen (H_2) to produce carbon monoxide (CO). This is the reverse water gas shift (RWGS) reaction, which produces CO and water. While CO_2 is highly stable chemically, CO is highly reactive. This makes it a valuable raw material for manufacture of other chemicals, including and especially liquid hydrocarbon fuels such as gasoline and diesel; this could be achieved via the well-known Fischer Tropsch synthesis which uses synthesis gas, a mixture of H_2 and CO, as its raw material. In this study, the RWGS reaction has been investigated via computer simulation in order to determine the best way to maximize the overall conversion of CO_2 to CO, i.e., to force the RWGS reaction toward as much CO production as possible. The endothermic RWGS reaction generally requires very high temperatures (>700°C) for increased conversion. Such temperatures present challenges related to further carbon emission (depending on the source of heat energy) and materials stability. However, an integrated separation and recycling system, possibly incorporating a pressure swing adsorption

(PSA) and/or membrane process, could separate and recycle unreacted CO_2 and H_2 gases back to the reactor inlet resulting in higher overall CO_2 conversion compared with other methods suggested in the literature.

1. Introduction

Climate change and Greenhouse gas (GHG) emission have caused more interests for launching Carbon Capture and Sequestration (CCS) plants globally. In the future, amount of captured CO_2 will be increased resulting in more availability and low cost. Consequently new innovations are necessary in order to convert cheap CO_2 to useful products instead of sequestration plans or storage in the oceans. The coal power plant production rate for CO_2 in Canada is more than 90 million metric tons per year while our transportation system emits approximately the same amount of CO_2 from petroleum based fuel. If the CO_2 emitted by power plants reacts with hydrogen (H_2) coming from water electrolysis powered by a sustainable energy, producing synthetic fuel can cover most of energy needed for the transportation sector. These processes can reduce our need for petroleum-based fuel and CO_2 emission by 50%. In the future, the most industries including coal power plants have to sequestrate CO_2 and provide the concentrated stream to avoid penalty for emission. Hydrogenation of CO_2 and producing the valuable and extremely active carbon monoxide (CO) is one of the most important approaches to reduce GHG effect and diminish resource consumption. This issue is feasible by the reaction named Reverse Water Gas Shift (RWGS) reaction.

In this study, the objective was to develop a method for economic conversion of CO_2 into CO via RWGS. The simulations have been carried out to incorporate several process scenarios to increase the overall conversion of CO_2 to CO and to identify the best process operating conditions for the RWGS reaction.

2. RWGS applications and advantages

The best known process for turning CO_2 into CO is RWGS, in which CO_2 reacts with hydrogen to produce CO and water as follows:

$$CO_2 + H_2 = CO + H_2O \qquad \Delta H = +41.12\ \text{kJ/gmol (endothermic)} \tag{1}$$

Leading process to make synthetic fuel is Fischer-Tropsch (F-T) that uses synthesis gas (a.k.a. syngas, a mixture of CO and H_2) coming from RWGS as feed and produces low sulfur liquid hydrocarbon that easily could be refined to various valuable products. The growing concern over CO_2 from high emitter industries like coal power plants has led over the years to much research into capturing CO_2 from exhaust flue gas. This raises the potential of enormous amounts of CO_2 becoming available as a raw material for the CO component of synthetic fuel. The production cost of one liter of gasoline through the RWGS-to-Fischer Tropsch process has been estimated at \$3, and if a \$30 per ton tax would be applied to CO_2 emissions, the cost could be decreased to as low as \$2 per gallon [Schultz et al., 2009]. Liquid fuel derived from CO_2 would easily integrate within the existing infrastructure since it is chemically almost identical to conventional petroleum-derived transportation fuel. It also has more energy density as well as ease of storage and transportation compared to competing hydrogen-based transportation fuel alternatives. There are a number of different known processes for converting CO_2 to valuable precursors. Methane dry reforming is one of the known technologies for conversion of CO_2 to CO and H_2. Although it is available in industrial scale, reduction of CO_2 via dry methane reforming still is questionable due to high energy consumption [Centi et al., 2009]. Moreover, methane is a fuel in great and growing demand today as a fuel in its own right and will likely rise in price. This introduces high up-front feedstock costs to a syngas production process. Therefore using methane to convert CO_2 cannot be a suitable option. Direct hydrogenation of CO_2 to other chemicals is another process for CO_2 conversion when CO_2 react with H_2 and produce product like methanol. Some promoted catalysts have been studied for direct hydrogenation of CO_2 to methanol [Joo et al., 1999]. However, one of the important problems for production of methanol via direct catalytic hydrogenation of CO_2 is water formation. On the surface of the catalyst, water can be an inhibitor and reduce activity for methanol formation. CO_2 tends to oxidize the catalyst more than CO does, and so reduces the activity of the catalyst for methanol production. By contrast, methanol production yield in CO_2 hydrogenation via RWGS process was twice as high as the yield in direct hydrogenation of CO_2 [Joo et al., 2004]. Methane production from CO_2 hydrogenation known as Sabatier reaction is another option for use of CO_2 as a raw material:

$$CO_2 + 4H_2 \rightarrow CH_4 + 2H_2O \tag{2}$$

But it requires significant H_2 to convert CO_2 via Sebatier than to do so via RWGS In addition, methane has lower energy value compared to liquid hydrocarbon fuels.

Therefore this process is a less attractive method for CO_2 conversion to valuable fuels than RWGS.

3. Different factors affecting CO_2 conversion in RWGS

Different factors affecting RWGS reaction, such as temperature, pressure, residence time and catalyst. Overall process efficiency depends on CO_2 conversion and should be maximized in order to produce valuable CO.

3.1. Kinetics and residence time in RWGS reactor

Kinetics of RWGS has been studied in the literature and it was found that mechanism could follow nearly chain-reaction model [Bustamante et al., 2004], [Wang et al., 2003]. RWGS reaction is a fast one and therefore the residence time in reactor must be kept low. Increasing the residence time twice has not shown significant effect on conversion and selectivity for CO production [Brooks et al., 2006]. In high flow rate, residence time will be less inside the reactor so more catalyst must be used; and in lower flow rate and higher residence time, mass transfer resistance should be considered because of lower Reynolds number [Whitlow and Parrish, 2001]. However, more studies are required to find kinetics and residence time effect under certain conditions and different catalysts.

3.2. Feed ratio (H_2/CO_2)

Experiments showed that in the RWGS reaction, hydrogen participation is the important factor for CO formation from CO_2. Increased hydrogen concentration increases CO_2

conversion compared to equimolar H_2 and CO_2 feed [Hu et al., 2007]. CO production can be significantly enhanced by increasing H_2/CO_2 ratio over Cu/SiO_2 catalyst [Chen et al., 2002]. But there are two constraints for H_2/CO_2 ratio, the first is the hydrogen availability and the second is the parallel Sabatier reaction resulting to methane production which is not desirable for the RWGS reaction. The best H_2/CO_2 ratio based on experiments could be between 1 and 2. Ratio of 1.2/1 showed very good conversion (97% of equilibrium) in the presence of suitable catalyst. The conversion to CO could be reduced (90% of equilibrium) by increasing the ratio to 2/1 due to various reasons such as heat transfer limit, mass transfer limit and some sequential reaction like Sabatier [Holladay et al., 2008]. Studies also showed that increased H_2/CO_2 ratio increased the conversion [Brooks et al., 2006]. However their results showed that for low residence times, increased H_2 might be an obstacle for CO_2 to reach to catalyst surface and therefore could decrease CO_2 conversion.

3.3. Catalyst

It has been reported that water gas shift (WGS) reaction catalysts can catalyze the RWGS reaction as well [Holladay et al., 2007]. But selecting a catalyst which can operate in high temperature with suitable life time is one of the main challenges in RWGS reaction. This reaction was studied on disulfides of molybdenum and tungsten. These catalysts showed lower activity compared to other transition metals such as Fe, Co and Ni, but selectivity toward CO was higher than transition metal catalysts. Ni-CeO_2 with 2wt.% Ni has been synthesized by co-precipitation and its activity for CO production and catalyst life time were excellent. CeO_2 was 100% selective to CO compared to Ni-CeO_2 which had CH_4 as by-product. But activity of the catalyst Ni-CeO_2 is higher than CeO_2, and this activity increases by increasing the Ni content till 2wt. %. It has been noticed that at higher Ni content (more than 5wt. %) CH4 yield increased as by-product. In terms of the stability, TOS (time on stream) analysis was studied for RWGS reaction over 2wt %Ni-CeO_2 for 9 hours continuously and it showed very good stability at $600^{o}C$ [Liu et al., 2008].

Also other Ce based catalysts have been studied for WGS. 5wt.%Au/20wt.%Ce/Al_2O_3 showed very good activity, and could be suitable for RWGS reaction [Gunes and Yildirim, 2010]. But further investigation for its stability should be done to achieve overall performance in industrial scale in addition to economical consideration. ZnO/Al_2O_3 catalyst would be suitable for RWGS though the activity is slightly lower than others [Park et al., 2001]. But, taking into consideration that by recycling the reactants, the conversion of CO_2 can be increased, this drawback could be compensated significantly. A pilot plant for methanol production was studied [Joo et al., 2004]. $ZnAl_2O_4$ activity has not decreased at $700^{o}C$ during 9 days of process indicating its stability compared to other commercial catalysts [Joo et al., 2004]. Ru/ZrO_2-CeO catalyst showed very high activity for RWGS in micro reactor by achieving near 97% of equilibrium at $800^{o}C$ [Holladay et al., 2008]. The activity of 6% Ru/CeO_2-ZrO_2 catalyst was near equilibrium conversion and it was reported to be a stable catalyst [Holladay et al., 2008].

4. Simulation results and discussion

Conversion of CO_2 via the RWGS reaction was simulated using the Unisim software package. Initially, a perfectly effective catalyst was assumed in order to ascertain complete expected conversions at different temperatures; RWGS is endothermic and conversion increases with temperature. Further, it was assumed that a separation system—also undefined at this stage—would separate 80 percent of the unreacted raw materials for recycling back to the RWGS reactor inlet. As other processes described in the literature utilized multiple reactors in order to increase overall CO_2 conversion [Doty et al., 2010], it was decided here to use only one reactor and to maximize conversion under that constraint. The reason for this decision was the desire to avoid the large energy requirement of multiple reheating and cooling of the stream between reactors. Moreover, by applying three reactors and two highly efficient heat exchangers, the overall conversion would not be more than 66% for CO_2 [Doty et al., 2010]. Hence, optimization of RWGS requires integrating a downstream separation process which could be efficient and cost effective. Here factors affecting overall conversion on CO_2 to CO are studied. Several options for recycling reactants and enhance the overall conversion of CO_2 have also been considered in this regard.

4.1. Temperature and Pressure effects

The RWGS is an endothermic, equilibrium-limited reaction which exhibits increased conversion with an increase in temperature. Unlike the water gas shift (WGS) reaction, which operates in the 150°C–300°C range, RWGS needs to be carried out at high temperature conditions, since as temperature increases, the equilibrium constant (Keq) will be increased. The K_{eq} of the RWGS reaction would be about 1 at 800°C, meaning higher temperatures are needed to shift the equilibrium and favor CO formation. Figure 1 shows the direct relationship between CO_2 conversion and temperature at a total pressure of 1 bar by UNISIM (process modeling software by Honeywell) simulations carried out.

Conversion is very low at temperatures less than 400°C due to lower K_{eq}. Also because of parallel, mostly exothermic reactions, regardless of reverse reaction (WGS), temperature inside the reactor must be kept within a particular range so that these other exothermic reactions don't affect the target products. Temperature cannot be so low as to enable parasitic reactions, and cannot be so high as to necessitate heat sources and expensive temperature resistant materials. Also there is limitation with respect to catalyst deactivation at high temperatures. Considering these limitations, the range between 750 and 800°C would be suitable.

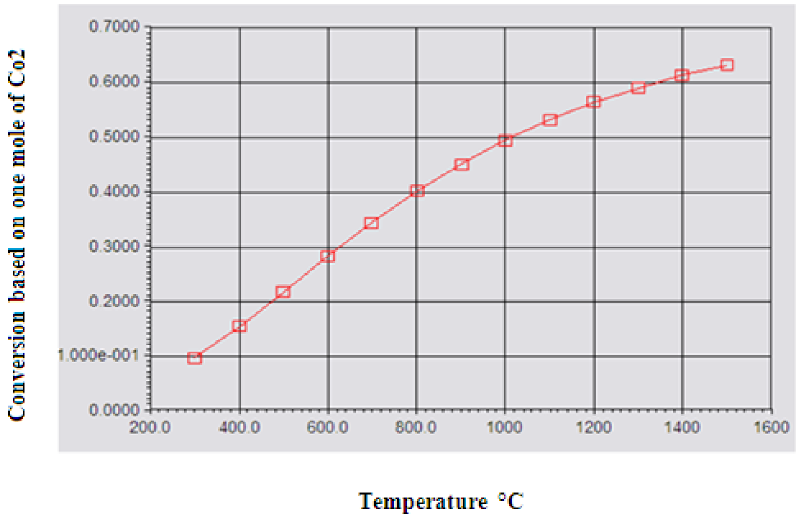

Figure 1: Relationship between temperature and CO_2 conversion at equilibrium calculated by UNISIM simulations.

Pressure could reduce activation energy under certain conditions [Bustamante et al., 2004]. The total moles of CO_2 and H_2 in RWGS reaction are equal to the total moles of CO and H_2O. Therefore pressure doesn't affect the CO_2 conversion significantly. The UNISIM simulations have proven this to be the case.

4.2. Separation of unreacted CO_2 and H_2

Asymmetric polyimide hollow fiber membrane for H_2 separation from CO has been tested by Peer et al, in 2007, and showed very good potential for separation of H_2 from CO [Peer et al., 2007]. However it is recommended to investigate membrane performance on syn gas containing CO_2 as well as CO. Also Brunetti et al introduced a membrane reactor (Pd–Ag), to separate H_2 from a syn gas containing CO 45%, H_2 50%; CO_2 4% and N_2 (dry basis) for fuel cell. The performance of membrane reactor showed good ability to separate H_2 from syn gas resulting in more H_2 recovery in water gas shift reaction [Brunetti et al., 2011].

First commercially available membrane for CO_2 removal from syn-gas containing carbon monoxide has been introduced by Membrane Technology and Research as MTR's unique Polaris™ membrane. This membrane can separate 80% of the CO_2 in stream by purity up to 95% in feed pressure of 800 psi. Membrane composed of thin film, composite polymer to increase the flux of CO_2 by permeability 10 times more than conventional membrane (cellulose acetate membrane) for CO_2 separation from methane [S. Shelley, 2009]. The COPure^{SM} process is the method which selectively separate CO by complexation/decomplexation of CO in a proprietary solvent containing cuprous aluminum chloride ($CuAlC1_4$) dissolved in an organic liquid such as toluene. Typical product recovery is 98%, and purity is 99% [Costello & Assoc., Inc].

A novel adsorption cycle was tested for recovering CO_2 from CO by means of zeolite NaY as an adsorbent. The stream contained equal moles of CO_2 and CO. Zeolite NaY showed high selectivity and capacity for CO_2 in the presence of CO [Walton and Le Van, 2006]. This process was designed and constructed as an innovative low energy and low mass device for recovering CO_2 and CO for the Mars in-situ resource utilization projects. Nevertheless, it could be a suitable process and cost effective method to separate CO_2 from syn gas, but particular tests are required to prove its efficiency in case of RWGS reactor outlet stream. For in-situ water removal by membrane reactor, silicone rubber/ceramic composite membrane reactor has been studied for the methanol synthesis from CO_2 and showed the efficiency of this type of reactor by in-situ removal of water and forcing the reaction toward producing CO and water [Chen and Yuan, 2004]. Membrane reactors can be very useful in the future if they can be improved specially in practical conditions and high temperatures. Currently it is very hard to trust them for long term applications in industrial scale due to many reasons such as high volume operations, stabilities, and toxicities of the components after a long time.

4.3. Simulation results

Proposed process for RWGS in this study contains a condenser for water removal and an integrated separation system including PSA and/or membrane downstream of the RWGS reactor. Water produced from RWGS must be removed due to its toxicity for the probable F-T or methanol production process catalyst after the RWGS reaction. Water can block the active sites and reduced the catalyst activity. Also it is easier to separate reactants from syn gas by lowering the amount of saturated water in the stream as much as possible. Figure 2 shows envisioned flow sheet for RWGS process simulated in UNISIM software. CO_2 and H_2 are mixed prior to the reactor. The RWGS reactor outlet stream will be cooled down and condensed in a condenser in order to remove water. Then gas mixture will be sent to a separation system to separate CO_2 and CO. Depending on the separation system, H_2 can pass through and be recovered. Unreacted CO_2 and H_2 will be recycled back to the reactor feed after compression and therefore amount of CO_2 which leaves the system could be reduced significantly. The rate of reactants and products for this process are shown in figure 2. Based on 100 kg-mole/hr of each reactant, 75 kg-mole/hr CO will be produced based on 80% of separation efficiency. Most water will be removed in condenser but depending on temperature and pressure, some saturated water could still be in stream.

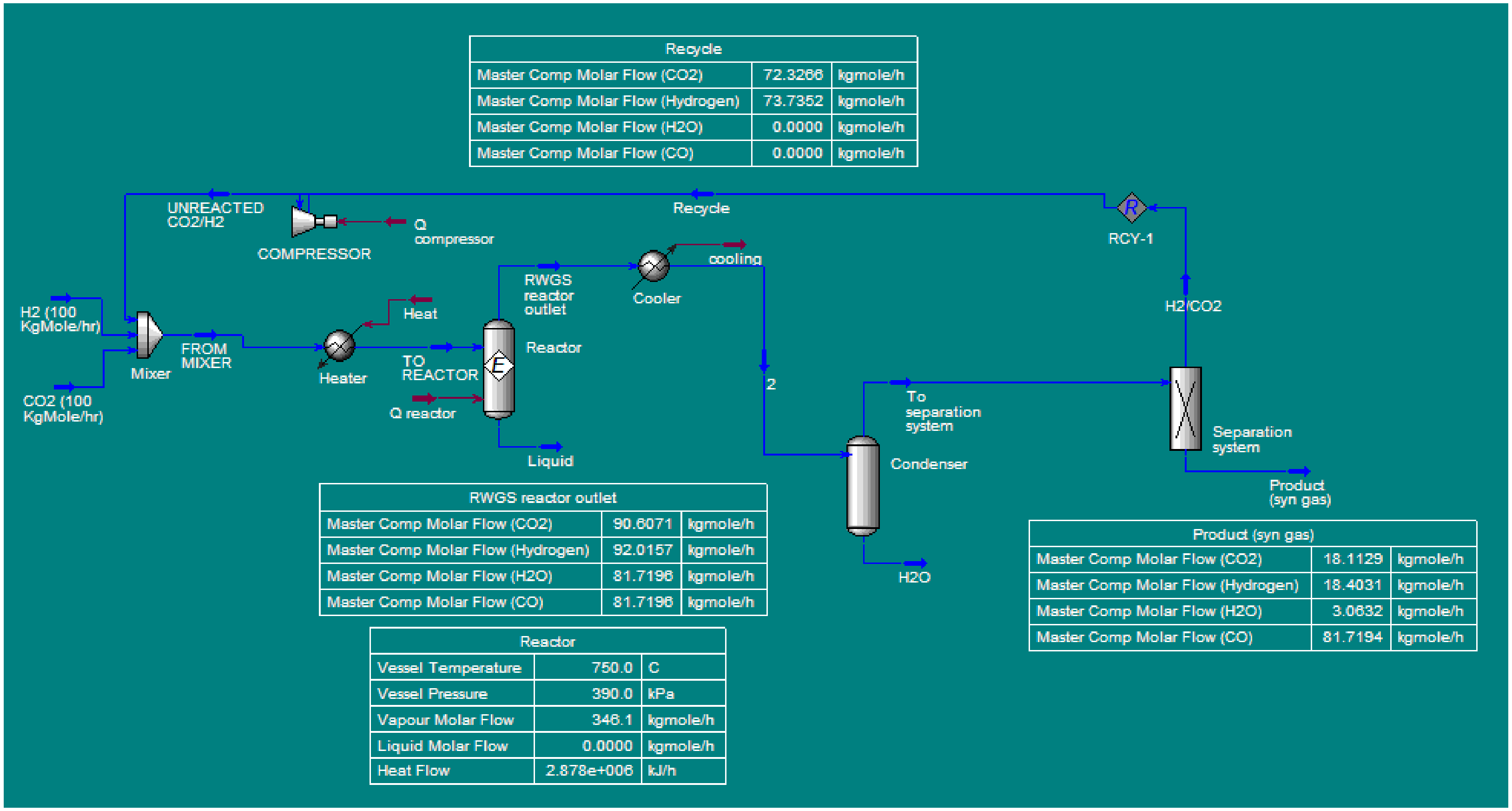

Recycle		
Master Comp Molar Flow (CO2)	72.3266	kgmole/h
Master Comp Molar Flow (Hydrogen)	73.7352	kgmole/h
Master Comp Molar Flow (H2O)	0.0000	kgmole/h
Master Comp Molar Flow (CO)	0.0000	kgmole/h

RWGS reactor outlet		
Master Comp Molar Flow (CO2)	90.6071	kgmole/h
Master Comp Molar Flow (Hydrogen)	92.0157	kgmole/h
Master Comp Molar Flow (H2O)	81.7196	kgmole/h
Master Comp Molar Flow (CO)	81.7196	kgmole/h

Reactor		
Vessel Temperature	750.0	C
Vessel Pressure	390.0	kPa
Vapour Molar Flow	346.1	kgmole/h
Liquid Molar Flow	0.0000	kgmole/h
Heat Flow	2.878e+006	kJ/h

Product (syn gas)		
Master Comp Molar Flow (CO2)	18.1129	kgmole/h
Master Comp Molar Flow (Hydrogen)	18.4031	kgmole/h
Master Comp Molar Flow (H2O)	3.0632	kgmole/h
Master Comp Molar Flow (CO)	81.7194	kgmole/h

Figure 2: Envisioned flow sheet for RWGS process by UNISIM

Figure 3 indicates CO_2 conversion as a function of temperature and CO_2 recycle ratio. As shown in this figure separation and recycling of CO_2 after reactor could compensate greatly for the effect of temperature on overall conversion. In this case by increasing the amount of recycled CO_2, need of high temperature in the reactor would be eliminated. In this 3-dimensional figure, the minimum conversion is at zero recycling. But as recycle ratio increases, conversion of CO_2 reaches to the maximum for all temperatures.

Figure 4 Shows the CO_2 conversion versus recycling of the H_2 and CO_2. It can be observed here that without recycle CO_2 conversion is around 39%, at 750^{o}C while recycling one of the components (CO_2 or H_2) results in an increase in CO_2 conversion up to 90%. Since the number of moles for each reactant is equal, there is no significant difference in overall conversion for recycling of CO_2 compared to H_2 individually. As it could be predicted, simulation showed that recycling of both components has the highest effect on overall CO_2 conversion up to 100%. Based on average temperature of 750^{o}C and integrated separation technology, even with only 80% of reactants being separated and recycled back to the reactor, conversion of CO_2 will be increased to 75% in the RWGS process without need of more reactors, catalysts and energy consumption for re-heating of the feed.

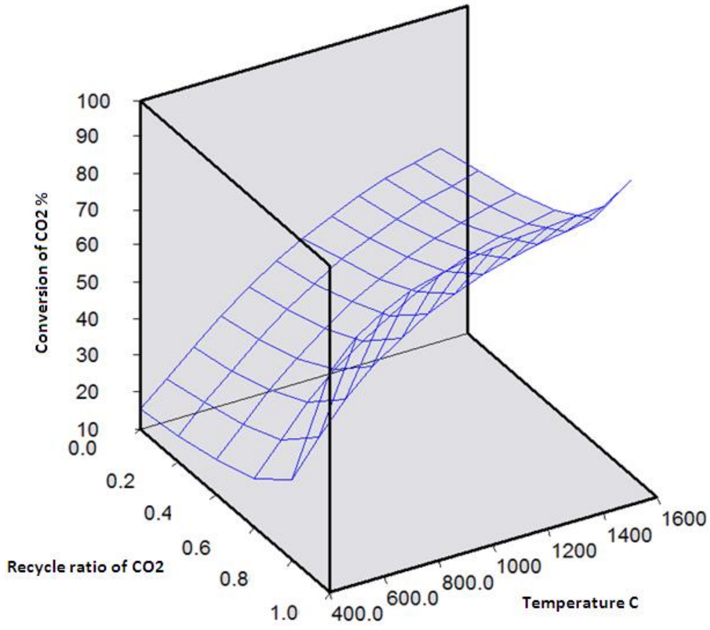

Figure 3: CO_2 conversion as a function of temperature and CO_2 recycle ratio for RWGS simulated by UNISIM software

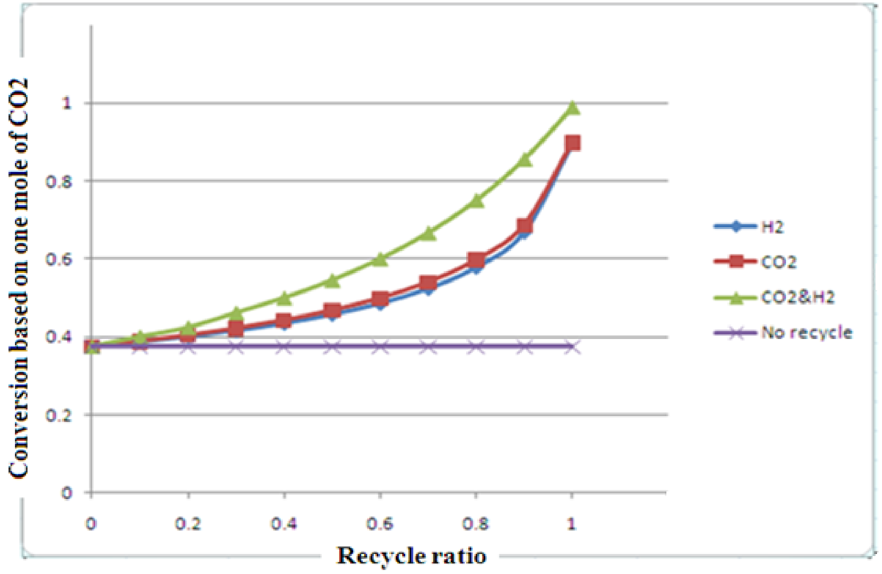

Figure 4: CO_2 conversion comparison by reactant recycle ratio and no recycle, at temperature 750°C

5. Conclusions

By carrying out UNISIM simulations, it was shown in this study, that as reaction temperature increases, the conversion of CO_2 to CO would increase, as expected for an endothermic reaction. Pressure did not have a significant effect on the conversion for this reaction. To increase the overall conversion of this process, separation and recycle of unreacted CO_2 and H_2 gases from RWGS reaction products (CO and H_2O) have been considered in this study. It was shown that conversion of CO_2 can be increased to 75% in the RWGS process without the need for more reactors. The energy consumption for the overall process can be decreased substantially by recycling the CO_2 and H_2 gases instead of increasing the temperature of the reactor to increase the overall conversion. Separation by a membrane unit, a pressure swing adsorption (PSA) or an integrated separation system after reactor is more efficient compared to the multistage reactor processes suggested in the literature in increasing the overall conversion of CO_2.

Acknowledgements

Authors would like to acknowledge the financial support received from NSERC (Natural Science and Engineering Research Council) of Canada and Phoenix Canada Oil company, Limited for this study.

6. References

Brooks, K., S. Rassat, J. Hu, S. Stenkamp, S. Schlahta, J. Bontha, J. Holladay, T. Simon, K. Romig and C. Howard (2006). "Development of a microchannel in situ propellant production system." Space Technology and Applications International Forum - STAIF 2006 **813**: 1111-1121.

Brunetti, A., G. Barbieri and E. Drioli (2011). "Integrated membrane system for pure hydrogen production: A Pd-Ag membrane reactor and a PEMFC." Fuel Processing Technology **92**(1): 166-174.

Bustamante, F., R. M. Enick, A. V. Cugini, R. P. Killmeyer, B. H. Howard, K. S. Rothenberger, M. V. Ciocco and B. D. Morreale (2004). "High-temperature kinetics of the homogeneous reverse water-gas shift reaction." Aiche Journal **50**(5): 1028-1041.

Costello. Rocky C, R.C. Costello & Assoc., Inc. COPureSM Carbon Monoxide Purification Technology http://www.rccostello.com/copure.html

Centi, G. and S. Perathoner (2009). "Opportunities and prospects in the chemical recycling of carbon dioxide to fuels." Catalysis Today **148**(3-4): 191-205.

Chen, C. S. and W. H. Cheng (2002). "Study on the mechanism of CO formation in reverse water gas shift reaction over Cu/SiO_2 catalyst by pulse reaction, TPD and TPR." Catalysis Letters **83**(3-4): 121-126.

Chen, G. W. and Q. Yuan (2004). "Methanol synthesis from CO_2 using a silicone rubber/ceramic composite membrane reactor." Separation and Purification Technology **34**(1-3): 227-237.

Doty, F. D., G. N. Doty, J. P. Staab and L. L. Holte (2010). "Toward efficient reduction of CO_2 to Co for renewable fuels." Es2010: Proceedings of Asme 4th International Conference on Energy Sustainability, Vol 1: 775-784.

Gunes, H. and R. Yildirim (2010). "Low temperature Water-Gas Shift Reaction on Au-CeO_2/Al_2O_3 catalysts." International Journal of Chemical Reactor Engineering **8**.

Holladay, J. D., K. P. Brooks, P. Humble, J. Hu and T. M. Simon (2008). "Compact reverse water-gas-shift reactor for extraterrestrial in situ resource utilization." Journal of Propulsion and Power **24**(3): 578-582.

Holladay, J. D., K. P. Brooks, R. Wegeng, J. Hu, J. Sanders and S. Baird (2007). "Microreactor development for Martian in situ propellant production." Catalysis Today **120**(1): 35-44.

Hu, J. L., K. P. Brooks, J. D. Holladay, D. T. Howe and T. M. Simon (2007). "Catalyst development for microchannel reactors for martian in situ propellant production." Catalysis Today **125**(1-2): 103-110.

Joo, O. S., K. D. Jung and Y. S. Jung (2004). "CAMERE Process for methanol synthesis from CO_2 hydrogenation." Carbon Dioxide Utilization for Global Sustainability **153**: 67-72.

Joo, O. S., K. D. Jung, I. Moon, A. Y. Rozovskii, G. I. Lin, S. H. Han and S. J. Uhm (1999). "Carbon dioxide hydrogenation to form methanol via a reverse-water-gas-shift reaction (the CAMERE process)." Industrial & Engineering Chemistry Research **38**(5): 1808-1812.

Park, S. W., O. S. Joo, K. D. Jung, H. Kim and S. H. Han (2001). "Development of ZnO/Al_2O_3 catalyst for reverse-water-gas-shift reaction of CAMERE (carbon dioxide hydrogenation to form methanol via a reverse-water-gas-shift reaction) process." Applied Catalysis a-General **211**(1): 81-90.

Peer, M., S. M. Kamali, M. Mahdeyarfar and T. Mohammadi (2007). "Separation of hydrogen from carbon monoxide using a hollow fiber polyimide membrane: Experimental and simulation." Chemical Engineering & Technology **30**(10): 1418-1425.

Schultz, K., S. L. Bogart, R. P. Noceti and A. V. Cugini (2009). "Synthesis of hydrocarbon fuels using renewable and nuclear energy." Nuclear Technology **166**(1): 56-63.

Shelley, S. (2009). "Capturing CO_2: Membrane systems move forward." Chemical Engineering Progress **105**(4): 42-47.

Walton, K. S. and M. D. LeVan (2006). "A novel adsorption cycle for CO_2 recovery: Experimental and theoretical investigations of a temperature swing compression process." Separation Science and Technology **41**(3): 485-500.

Wang, G. C., L. Jiang, Y. H. Zhou, Z. S. Cai, Y. M. Pan, X. Z. Zhao, Y. W. Li, Y. H. Sun, B. Zhong, X. Y. Pang, W. Huang and K. C. Xie (2003). "Investigation of the kinetic properties for the forward and reverse WGS reaction by energetic analysis." Journal of Molecular Structure-Theochem **634**: 23-30.

Wang, L. H., S. X. Zhang and Y. A. Liu (2008). "Reverse water gas shift reaction over co-precipitated Ni-CeO_2 catalysts." Journal of Rare Earths **26**(1): 66-70.

Whitlow, J. E. and C. F. Parrish (2003). "Operation, modeling and analysis of the reverse water gas shift process." Space Technology and Applications International Forum - Staif 2003 **654**: 1116-1123.

Chapter III: An experimental adsorbent screening study for separation of CO_2 from CO

Farhang Abdollahi(1), F. Handan Tezel(1), Stephen Aplin(2)

(1) University of Ottawa, Department of Chemical and Biological Engineering, Ottawa, ON, Canada

(2) The HDP Group, Ottawa, ON, Canada

Keywords: Pure gas isotherm, adsorbent screening, CO_2/CO separation

Abstract

Conversion of CO_2 to CO through Reverse Water Gas Shift (RWGS) reaction in order to reduce greenhouse gas (GHG) emission and produce valuable active CO gas could be an important alternative for carbon sequestration processes. In order to enhance this conversion, a separation system downstream of the RWGS reactor could recycle back un-reacted CO_2 to reactor. The present study has focused on finding a promising adsorbent for separation of CO_2 and CO in downstream of RWGS reactor. Adsorption equilibrium isotherm data have been obtained for CO_2 and CO for zeolite NaY, zeolite 4A, zeolite 13X, activated carbon F-600 at 3 different temperatures (313K, 343K and 373K) for pressures up to 5 atm. Isotherm experimental data were fitted by Langmuir and Toth equations. Adsorption activities have been studied by determining the isosteric heat of

adsorption, Henry's law constant, selectivity and expected working capacities in order to screen all the adsorbents. Zeolite NaY has been found to be the most suitable adsorbent among the ones that were studied for CO_2 and CO separation due to its selectivity and isosteric heat of adsorption.

1. Introduction

The emission of Greenhouse Gases (GHG) including carbon dioxide (CO_2) from coal power plants is the main drawback of this type of power plant. Their long term environmental effects are forcing legislation to penalize high CO_2 emission industries in the near future. Adsorption for the separation of CO_2 from flue gases has been studied for years and there are many suggestions in terms of CO_2 separation from mainly nitrogen exhaust gases. But, there remains a question as to what to do with the captured CO_2. Carbon sequestration and storage (CCS) is one of the solutions, but it is not a long term alternative because of high cost and uncertainties in long term application. Converting CO_2 to valuable products can be another option and it has been considered in different ways.

The most flexible chemical that could be derived from CO_2 is carbon monoxide (CO). It can be used in different processes to produce wide range of chemical products. Using the conventional Fischer-Tropsch process, the CO would react with H_2 to produce synthetic fuel. The reaction of CO_2 with H_2 (which could be provided from renewable sources like water electrolysis) is called Reverse Water Gas Shift (RWGS) reaction:

$$CO_2 + H_2 \rightarrow CO + H_2O \tag{1}$$

In order for this reaction to be feasible, H_2 should be provided from renewable sources like water electrolysis using renewable energy, such as solar. CO and water will be produced by the RGWS reaction. The main issue for CO_2 utilization in a RWGS process is the high energy consumption of reaction since RWGS is an endothermic reaction, for which conversion increases with increasing temperature. Therefore, high CO_2 conversion cannot be achieved at lower temperatures.

In this study, the possibility of separating the unreacted CO_2 and H_2 from reaction products CO and H_2O is considered, for their recycle back into the RWGS reactor will increase the overall conversion of CO_2 to CO. In our previous studies, it has been established that recycle of the unreacted CO_2 and H_2 into the RWGS would increase the overall conversion up to 75% (Abdollahi, et al., 2012), which is more than other suggested processes such as multi stages reactors, which increase the conversion up to 66% (Doty et al., 2010).

Recycling will require separating reaction products from unreacted raw materials, either in situ or downstream of the RWGS reactor. Separation is the opposite of mixing (which is favoured by the Second Law of Thermodynamics), and therefore difficult and potentially costly. Pressure swing adsorption is an efficient process for gas separations which could be one of the most cost effective processes for the CO_2 and H_2 separation. Thus, it has been considered for this application in this study.

2. Literature Review

Separation of CO_2 from CO by means of adsorption has not been studied much in the literature. Cu-based zeolites showed better selectivity toward CO adsorption rather than CO_2, but CO/CO_2 selectivity has been reported close to unity at 1 atm (Ma et al., 2010). Previous studies showed that Silicalite-1 has low adsorption capacity for CO_2 (Wirawan and Creaser, 2006a). Metal organic frameworks (MOF) have great surface area and high CO_2 adsorption. But most experiments for CO_2 adsorption on MOFs have shown their feasibility at high pressures (Sayari et al., 2011). Due to their small pore size compared to commercial zeolites, they could not be good adsorbents at lower pressures. Furthermore, currently they are expensive and in industrial scale so that they could not compete with available commercial adsorbents in terms of being cost-effective. Faujasite-type zeolites have been regarded as promising zeolites in industries for gas adsorption. In faujasite-type zeolites the SiO_2/Al_2O_3 ratio is an important factor for CO_2 adsorption. Many studies showed that zeolites with lower SiO_2/Al_2O_3 ratio had more CO_2 adsorption capacity due to their quadropole moment interactions with the corresponding heterogeneous surface of the zeolite with high Al_2O_3 content (Maurin et al., 2005; Harlick and Tezel, 2004; Walton and LeVan, 2006; Shao et al., 2009; Mulgundmath et al., 2012). In all cases, saturated stream requires to be dried as much as possible prior to adsorption column since water could compete for adsorption sites due to the hydrophilicity of the materials (Sayari et al., 2011). Table 1 presents summary of the CO_2 and CO gases adsorption capacities of different adsorbents studied in the literature.

Table 1: Literature summary of CO_2 and CO adsorption on different adsorbents

Adsorbent	Temperature (K)	Pressure (atm)	CO_2 adsorption capacity (mmol/g)	CO adsorption capacity (mmol/g)	References
13X	298	0.8	3.7	0.35	(Walton and LeVan, 2006)
13X	308	1	5.5		(Cavenati et al., 2004)
13X	313	1	4.5		(Ko et al., 2003)
13X	295	1	4.6		(Harlick and Tezel, 2004)
13X	298	1		0.5	(Saha and Deng, 2009)
NaY	298	0.8	4	0.2	(Walton and LeVan, 2006)
NaY	295	1	4.1		(Harlick and Tezel, 2004)
NaY	303	0.6	4.9	0.6	(Xie et al., 1996)
5A	298	0.8	3	0.7	(Walton and LeVan, 2006)
5A	298	1		1.2	(Saha and Deng, 2009)
5A	303	1.2	3.0	1.0	(Pakseresht et al., 2002)
4A	313.15	1	3	-	(Ahn et al., 2004)
Activated carbon	288	1	2.5		(Chue et al., 1995)
Activated carbon	317.4	1	2.94		(Berlier and Frere, 1996)

Based on their ideal selectivity (CO_2/CO), zeolite NaY, zeolite 13X and zeolite 4A were selected and screened in this study as potential candidates for CO_2 and CO separation by adsorption. Also activated carbon was tested because of its availability and thermal stability for the adsorbent screening for CO_2/CO separation. Adsorption equilibrium data is an important tool in order to find the most appropriate adsorbent as well as for the design of pressure swing adsorption process. In order to have more precise data for practical application, equilibrium data must be obtained over a wide range of operating temperatures (Lee et al., 2002). Pure gas isotherms data for each adsorbent were obtained and correlated with Langmuir and Toth models. In terms of separation ability each adsorbent have been compared for both CO_2 and CO. Finally the most suitable adsorbents were chosen for further studies which are adsorption behaviour and design of pressure swing adsorption for real gas mixture (CO_2, CO, H_2 and water) downstream of RWGS reactor. Moreover, the Temperature-Dependent Langmuir and Toth have been developed by various temperature experimental data in order to predict isotherm in different temperatures. Binary adsorption prediction for selected adsorbent was calculated prior to further experiments with ternary mixture.

3. Materials and Experimental Details

Both CO_2 and CO gases (99.9 wt.% purity) were obtained from Linde Canada (Burlington, Ontario). Table 2 shows the characteristics of CO_2 and CO gases studied as adsorbates in this study.

Table 2: characteristic of CO_2 and CO

Adsorbate	**Kinetic diameter (Å)** [1]	**Quadrupole moment (C m^2)** [2,3]	**Dipole moment (D)**[4]	**Polarizability (A^{o3})** [5]
CO_2	3.30	4.6×10^{-31}	-	2.24
CO	3.70	-8.37×10^{-40}	0.122	1.84

[1] (Beck, 1974) [2] (Chetty and Couling, 2011) [3] (Harries, 1970) [4] (Scuseria et al., 1991) [5] (Cai et al., 1987)

The characteristics of the selected adsorbents in this study are shown in Table 3. Figure 1 show a schematic diagram of the constant volume system which was used to determine pure component adsorption equilibrium capacities for different adsorbents at different pressures and temperatures.

Table 3: Properties of selected adsorbents for CO_2 and CO adsorption in this study

Adsorbent	**Supplier**	**Pellet**	**Surface area (m^2/g)**	**Particle Length (mm)**	**Average Pore diameter (nm)**	**Mean Particle Diameter (mm)**	**SiO2/Al2O3 ratio**	**Mesh size**
Zeolite 13X	Aldrich Co.	1/16	726	-	0.8	1.5	2.2	-
Zeolite NaY	UOP, USA	Rod	-	2.659	0.8	-	5.1	-
Zeolite 4A	W. R. Grace, Davison, USA	1/16	600-800	-	0.4	-	1.0	-
Activated carbon F-400	Calgon, Mississauga, ON	Granule	1052	-	-	0.55-0.75	-	12×40
Activated carbon F-600	Calgon, Mississauga, ON	Granule	906	-	-	1.0	-	12×40

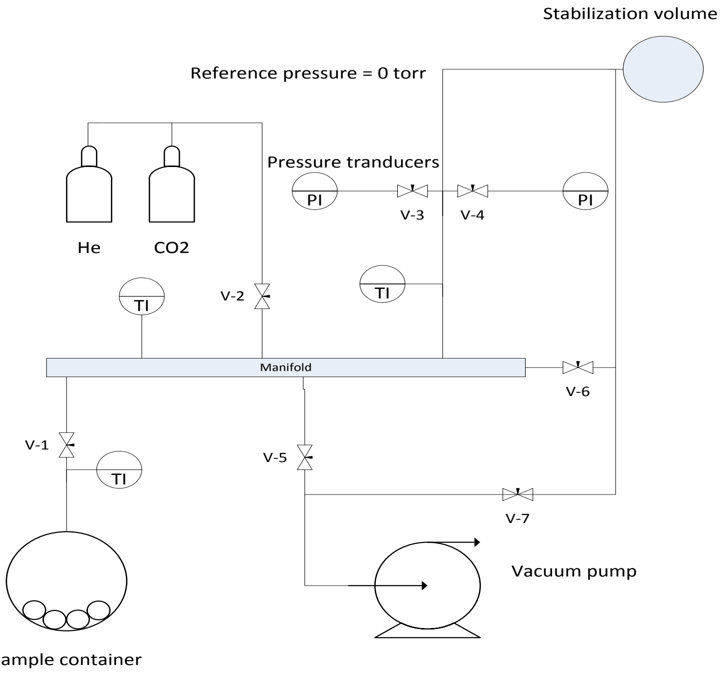

Figure 1: Schematic diagram of the constant volume system used in this study to determine pure component isotherms.

Pure gas adsorption isotherms of different adsorbents have been investigated by using two constant volume adsorption systems. Each of them are equipped with two pressure transducers for low (1000 torr) and high (160 pisa) pressures and three thermocouples for manifold, sample and room temperature. Working temperature range of these units was from 293K to 600K.

To carry out the experiments for adsorption isotherms, the required amount of adsorbent was first weighed, and then placed in the sample container. Adsorbents were regenerated for at least 10 hours at the regeneration temperature of 523K and 623K, for activated carbon and zeolites, respectively under vacuum pressure in order to degas and remove the moisture and other components that may be adsorbed in the adsorbent samples. The free volume of container after adsorbent loading was measured by helium assuming that it was not being adsorbed. Adsorbate gas was introduced into the dosing manifold first. When pressure stabilized in the manifold, it was measured as well as temperatures at different parts of the system resulting in determining the initial moles by ideal gas law. Then this gas was then allowed to enter into the sample container. Due to the expansion of the gas into the sample container, as well as due to adsorption of the gas into the adsorbent, there would be pressure drop in the system, which was measured by the pressure transducer. After achieving equilibrium, which was indicated by the stabilization of the pressure in the system, moles of adsorbed gas could be calculated from the PVT relationship. Data acquisition was carried out by using National Instruments based Lab-view v6.1 software on an Intel based desktop computer.

4. Theory

4.1. Isotherm models

The equilibrium isotherm data for pure gas adsorption of CO_2 and CO on various adsorbents were obtained at three different temperatures (313K, 343K and 373K) and pressures up to 5 atm. Then these data points were fitted using the Langmuir and Toth isotherm models. The Langmuir isotherm is based on monolayer adsorption by the following equation:

$$\frac{q}{q_s} = \frac{bp}{1 + bp} \tag{2}$$

In this equation q is the quantity of gas adsorbed, q_s is the maximum amount of gas adsorbed at saturation, b is the constant in Langmuir equation related to affinity between adsorbate and adsorbent, and p is the pressure of the system. Toth isotherm model has suitable behaviour in both low and high pressure and describes adsorption with sub-monolayer coverage. Toth model is presented by equation 3 (Toth, 1995):

$$\frac{q}{q_s} = \frac{bp}{[1 + (bp)^t\,]^{\frac{1}{t}}} \tag{3}$$

In this equation, t indicates the heterogeneity of the adsorbent. As t approaches unity the Toth isotherm model will be converted to Langmuir isotherm model. If it gets farther away from unity the system is more heterogeneous. Adsorption is dependent on temperature as it is an exothermic process. Increasing of temperature reduces adsorption capacity. Therefore temperature must be taken into account for predicting of adsorption behaviour. In order to predict the adsorption of CO_2 at different temperatures and pressures, the temperature–dependent Langmuir isotherm was selected to represent adsorption isotherms in this study. In Langmuir model q_s and b can be presented by following equations to become temperature-dependent parameters (Kikkinides et al., 1993):

$$q_s = k_1 - k_2 T \tag{4}$$

$$b = k_3 exp \left(k_4 / T \right) \tag{5}$$

In these equations k_1 (mmol/g), k_2 (mmol/g/K), k_3 (atm^{-1}) and k_4 (K) for pure gas isotherms have been obtained by correlating experimental data with the Langmuir model at the different temperatures. Also parameters of Toth (q_s, b and t) as functions of temperature can be expressed based on the following equations:

$$q_s = q_{so}\, exp \left[\chi \left(1 - T_o / T\right) \right] \tag{6}$$

$$b = b_o\, exp \left[Q / RT_o \left(T_o / T - 1 \right) \right] \tag{7}$$

$$t = t_o + \alpha \left(1 - T_o / T\right) \tag{8}$$

Where Q represents isosteric heat of adsorption and R is gas constant. Determination of the parameters for temperature-dependent form of the Langmuir and Toth isotherms has been done by means of a nonlinear regression routine. All data at three different temperatures were considered. Generalized Reduced Gradient (GRG2) nonlinear optimization method was implemented for this approach by the solver which is an enhanced version of Lasdon and Waren's GRG2 method. Final determination was accomplished when the absolute minimum sum of square residuals was obtained. In order to obtain deviation (DQ), following equation was applied where n is number of data points:

$$DQ = \frac{\sum_0^n 100 \times [\frac{q_{exp} - q_{cal}}{q_{exp}}]^2}{n} \quad (9)$$

4.2. Henry's law constant and isosteric heat

Henry's law constant could be determined by Toth model at low pressures as follows:

$$K_p = q_s . b \quad (10)$$

Isosteric heat of adsorption could be helpful to determine interactions between adsorbate-adsorbent and it is related to adsorption strength. It could be used as a parameter for measuring the energetic heterogeneity of adsorbent surface (Lee et al., 2002). Based on ideal Langmuir model, if the adsorbent surface is homogenous, the isosteric heat of adsorption must be independent of adsorbed loading. However this independence is seldom observed in reality since the interactions between adsorbate-adsorbent and the heterogeneity of the adsorbent surface are not negligible. High isosteric heat causes increase in temperature through PSA bed resulting in decrease in the adsorption capacities of gases and in the process efficiency. Therefore by measuring isosteric heat of adsorbent, one can determine how much heat should be removed from the PSA column to keep the temperature constant during the process. The isosteric heat of pure gas adsorption at zero fractional loading can be calculated by Clausius–Clapeyron equation:

$$\left(\frac{\Delta H_{iso}}{R}\right) = \left(\frac{\partial \, ln \, P}{\partial \left(\frac{1}{T}\right)}\right)_q \qquad (11)$$

Change in pressure P, as a consequence of change in temperature while amount adsorbed (q) is kept constant is related to isosteric heat in this equation. Isosteric heat can be obtained from the slope of the plot ln(P) versus 1/T at constant q.

4.3. Multicomponent mixture prediction

The Langmuir model can be extended to multicomponent gas adsorption for the prediction of mixture adsorption behaviour. Parameters obtained from pure component adsorption can be used in the following equation to predict the competitive adsorption of the components:

$$q_i = \frac{q_{si} . b_i . p_i}{[1 + \sum_{k=1}^{N} b_k . p_k]} \qquad (12)$$

In this equation q_i is the equilibrium amount of gas adsorbed for component i in the mixture, bi and q_{si} are Langmuir constants that could be obtained from pure component adsorption data and p_i is the partial pressure for component i in the mixture.

4.4. Selectivity

Selectivity factor is an important parameter in order to evaluate separation performance of adsorbents for two components. An ideal selectivity is calculated by dividing the amount of adsorbed CO_2 over CO (q_{co_2}/q_{co}) at the same temperature and pressure by assuming that there is no interaction between these two components. From binary mixture prediction data, the selectivity of adsorbents for components i and k could be defined as follows:

$$S_{i,k} = \frac{x_i/y_i}{x_k/y_k} \qquad (13)$$

where y is the mole fraction of component in the gas phase and x is the mole fraction in the adsorbed-phase. In adsorption by increasing temperature, selectivity will be decreased.

4.5. Expected working capacity

Adsorption capacity is a common parameter to determine the potential of adsorbents and indicates the amount of adsorbed gas at the feed cycle. Desorption of the component in the blow-down step is as important as the adsorption capacity since the component must be regenerated. The expected working capacity could be calculated by the difference between the amount of adsorbed gas at the feed cycle and at the blow-down cycle. Expected working capacity in this study has been calculated based on the pure gas isotherm. There are three methods of desorption in regeneration cycle such as Pressure Swing Adsorption (PSA), Temperature Swing Adsorption (TSA) and Pressure Temperature Swing Adsorption (PTSA). Working capacity could be different in the reality because desorption is endothermic and temperature will be decreased across the adsorption bed during blow-down step resulting to reverse adsorption and lower desorption. In this study, the effect of temperature change has been considered negligible so that expected working capacity is an ideal working capacity rather tha adiabatic working capacity. However, the expected working capacity could be a useful parameter to identify the most suitable adsorbent and process related to the operating conditions. Equation 12 defines expected working capacity, EWC as the difference in adsorption capacity at feed conditions and at blow-down conditions, as follows:

$$EWC = q\left(P_f, T_f\right) - q(P_b, T_b) \tag{14}$$

In this equation, P_f, P_b, T_f and T_b are pressure and temperature at the feed and blow-down steps respectively.

5. Results and discussion

5.1. Pure gas isotherms at different temperatures

Pure gas isotherms at three different temperatures and at pressures up to 5 atm have been determined for activated carbon F-600, zeolite 4A, zeolite NaY, and zeolite 13X. Figure 2 shows adsorption isotherms of pure CO_2 and CO gases for these adsorbents at various temperatures as a function of pressure. T-D Toth and Langmuir isotherm models have been used to fit these adsorption isotherms for each adsorbent. Tables 4 and 5 present parameters for temperature dependent Langmuir and Toth adsorption isotherm models and Table 6 lists Langmuir and Toth parameters at different temperatures for zeolite NaY.

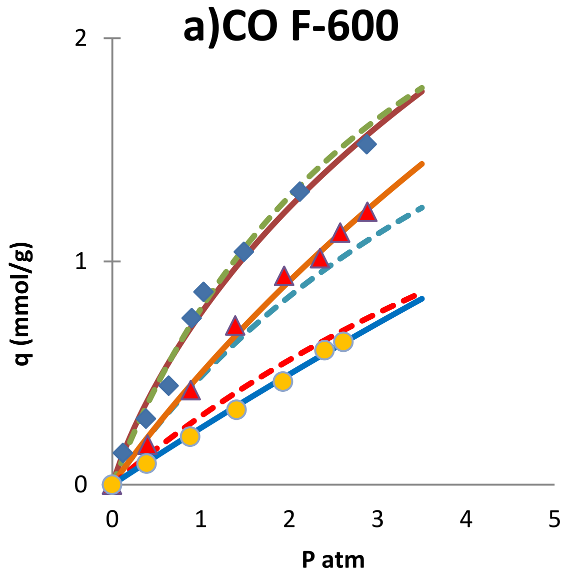

a)CO F-600

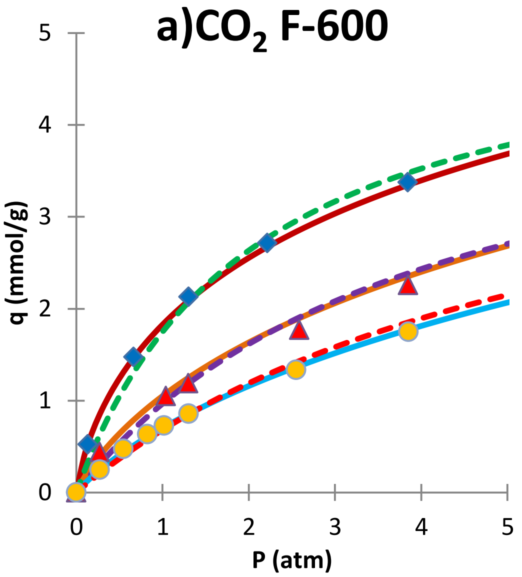

a)CO_2 F-600

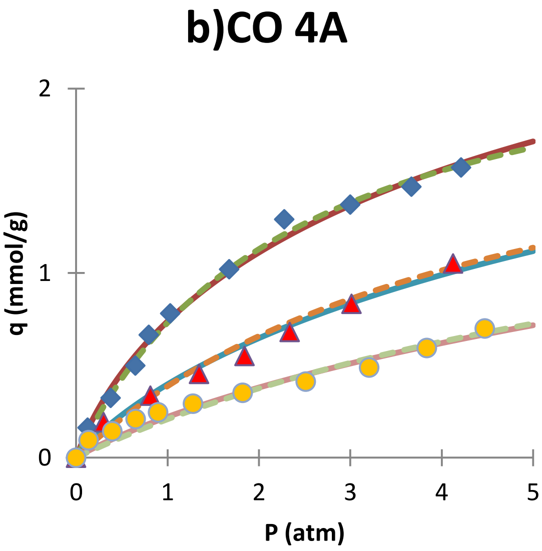

b)CO 4A

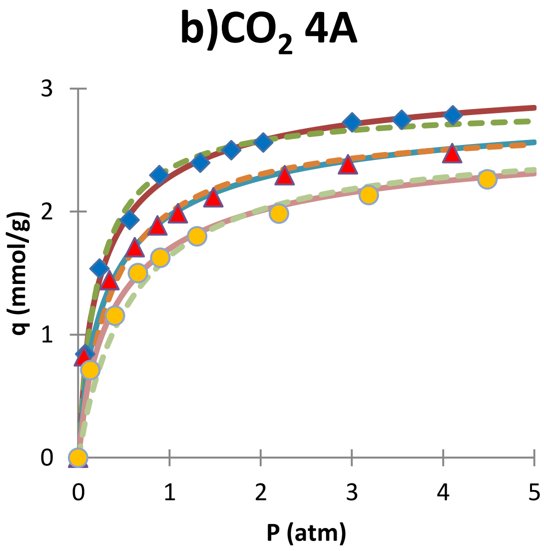

b)CO_2 4A

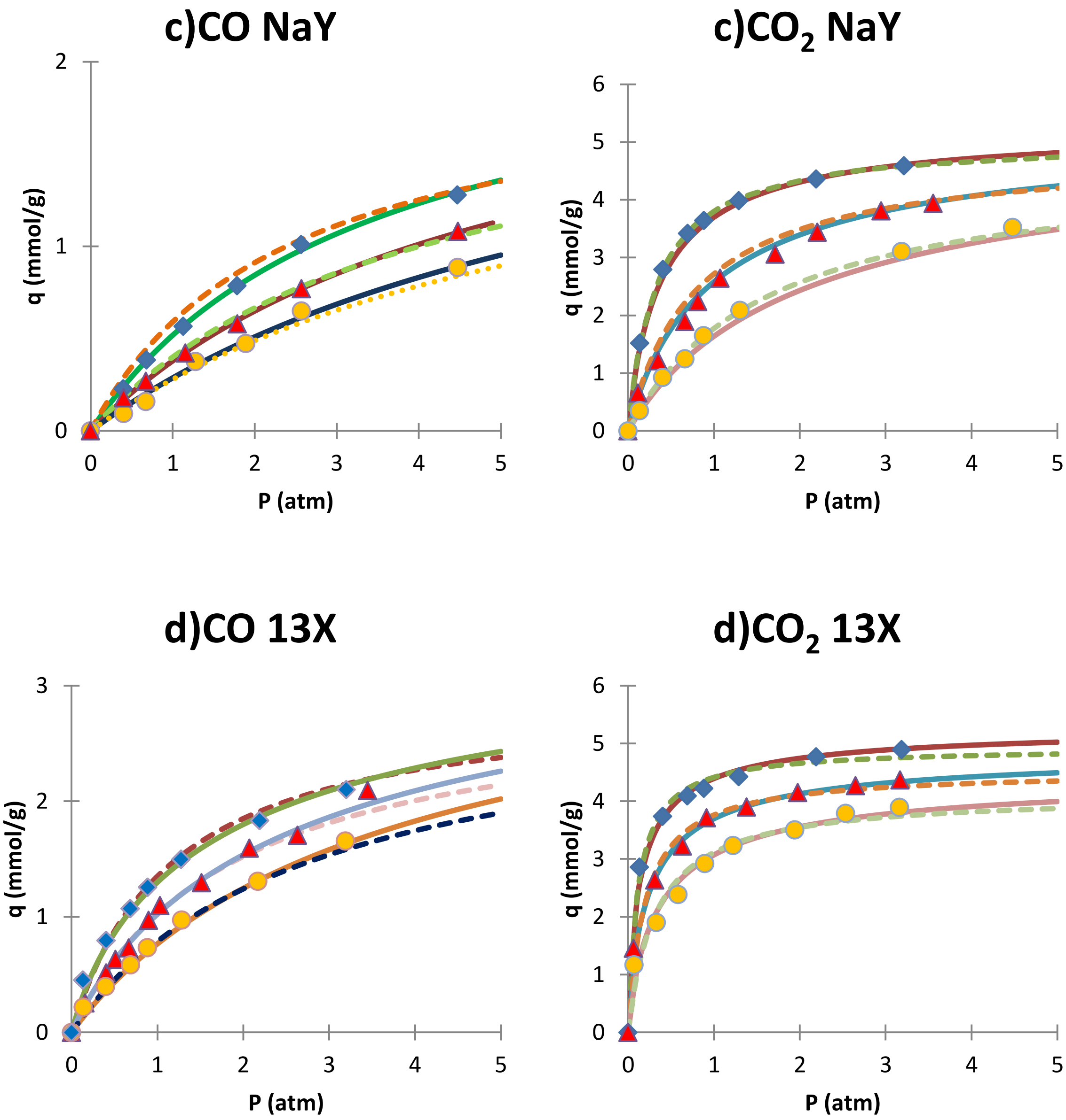

Figure 2: Adsorption isotherms of CO_2 and CO for 4 adsorbents studied.

a) AC F-600
b) Zeolite 4A
c) Zeolite NaY
d) Zeolite 13X

(♦) 313K
(Δ) 343K
(•) 373K

(- - - - -) Langmuir
(———) Toth

Table 4: Temperature-dependent Langmuir Isotherm Parameters for CO_2 and CO with 4 adsorbents looked at in this study.

Parameters	**Zeolite NaY**		**Zeolite 13X**		**Zeolite 4A**		**AC F-600**	
	CO_2	**CO**	**CO_2**	**CO**	**CO_2**	**CO**	**CO_2**	**CO**
k1 (mmol/g)	7.07	1.99	9.10	2.93	4.22	8.00	8.50	5.97
k2 (mmol/g/K)	0.006	0	0.013	0	0.004	0.016	0.010	0.007
k3 (atm^{-1})	1.51E-04	0.0011	0.0143	0.0044	1.04E-02	2.35E-07	0.0012	0.0007
k4 (K)	3097.84	1850.03	2000.13	1641.26	2000.12	2398.68	1850.06	1850.05
DQ	0.50	2.61	1.02	1.19	1.40	3.21	1.11	2.15

Table 5: Temperature-dependent Toth Isotherm Parameters for CO_2 and CO with 4 adsorbents looked at in this study.

Toth parameters	**Zeolite NaY**		**Zeolite 13X**		**Zeolite 4A**		**AC F-600**	
	CO_2	**CO**	**CO_2**	**CO**	**CO_2**	**CO**	**CO_2**	**CO**
q_{so} **(mmol/g)**	5.29	2.32	6.17	3.62	3.57	4.13	10.35	10.90
b_o **(atm^{-1})**	2.93	0.29	67.83	0.83	15.34	0.38	0.82	0.13
$^{Q}/_{RT_o}$	10.8	4.45	13.03	6.76	5.15	9.80	11.3	10.4
t_o	0.897	0.98	0.42	0.74	0.50	0.59	0.42	0.49
α	0	0	0.13	1.1893	0	0	0.609	2.962
χ	0	0	0	0	0.55	0.24	0	0.15
DQ	0.29	0.43	0.16	0.79	0.23	2.27	0.16	0.75

Table 6: Langmuir and Toth coefficients at different temperatures for CO_2 and CO adsorption on zeolite NaY

Adsorbent	**GAS**	**T(K)**	**Langmuir**		**Toth**		
			q_{sL}(mmol/g)	**b_L (atm^{-1})**	**q_{sT}(mmol/g)**	**b_T(atm^{-1})**	**t**
Zeolite NaY	**CO_2**	313	5.06	3.00	5.29	2.93	0.89
		343	4.86	1.26	5.29	1.13	0.89
		373	4.67	0.611	5.29	0.51	0.89
	CO	313	1.99	0.419	2.32	0.29	0.98
		343	1.99	0.250	2.32	0.19	0.98
		373	1.99	0.162	2.32	0.14	0.98
Zeolite 13X							
	CO_2	313	4.92	8.57	6.17	67.83	0.42
		343	4.52	4.90	6.17	21.69	0.43
		373	4.12	3.06	6.17	8.33	0.44
	CO	313	2.93	0.85	3.62	0.83	0.74
		343	2.93	0.53	3.62	0.46	0.85
		373	2.93	0.36	3.62	0.28	0.93
Zeolite 4A							
	CO_2	313	2.85	4.65	3.57	15.34	0.50
		343	2.73	2.66	3.39	9.77	0.50
		373	2.61	1.66	3.21	6.69	0.50
	CO	313	2.48	0.41	4.13	0.382	0.59
		343	2.20	0.21	4.04	0.16	0.59
		373	1.92	0.12	3.94	0.078	0.59
AC F-600							
	CO_2	313	5.32	0.48	10.35	0.82	0.42
		343	4.91	0.24	10.35	0.22	0.49
		373	4.65	0.17	10.35	0.11	0.52
	CO	313	3.57	0.28	10.90	0.13	0.49
		343	3.34	0.16	10.74	0.053	0.75
		373	3.11	0.10	10.58	0.024	0.97

The experimental data in general were better represented by the Toth model, compared to the Langmuir. For all the adsorbents looked at in this study, CO_2 was adsorbed much more than CO. In the literature, CO_2 showed competitive adsorption compared to CH_4 and N_2 on ZSM-5 zeolite due to its high polarizability and quadrupole moment (Harlick and Tezel, 2002). The high adsorption capability for CO_2 was reported with BaZSM-5 zeolite because of its higher polarity and acidity compared to CO (Wirawan and Creaser, 2006b). In this study, it can be seen that CO_2 was adsorbed much more since it has more quadrupole moment and polarizibility than CO. Also zeolite 13X has very good activity for CO_2 adsorption and this is in good agreement with literature (Lee et al., 2002; Harlick and Tezel, 2004; Zhang et al., 2008; Merel et al., 2008).

As can be seen from Figure 2, CO adsorption keeps increasing at higher pressures, as CO_2 adsorption starts to level off for all the adsorbents looked at in the present study. Therefore, pressure must be chosen as low as possible in order to maximize the selectivity for CO_2/CO separation. CO isotherm with AC F-600 is much more linear compared to zeolites studied. Figure 3 compares the adsorption isotherms of CO_2 and CO for all adsorbents at 313K for pressures up to 5 atm. Only Toth isotherm model was shown in this figure; experimental data points were not shown not to crowd it. This temperature has been chosen due to process conditions for CO_2 and CO separation downstream of RWGS reactor. As shown in figure 3 CO_2 and CO adsorption capacities on zeolite 13X are the highest compared to other adsorbents. It must be noticed that in despite of good adsorption capacity for CO_2, zeolite 13X has the highest adsorption capacity for CO as well. The low SiO_2/Al_2O_3 ratio of this adsorbent appears to favour more CO_2 adsorption. Higher SiO_2/Al_2O_3 ratio can cause less active cationic adsorption sites on adsorbent surface resulting lower amount of adsorption (Harlick and Tezel, 2004). It is well known that in order to separate CO_2 from CO, the most important factor is the difference between the adsorption capacities of these two components. As it can be seen from Figure 3, Zeolite NaY has shown the lowest CO adsorption capacity at 313K among all the adsorbents studied.

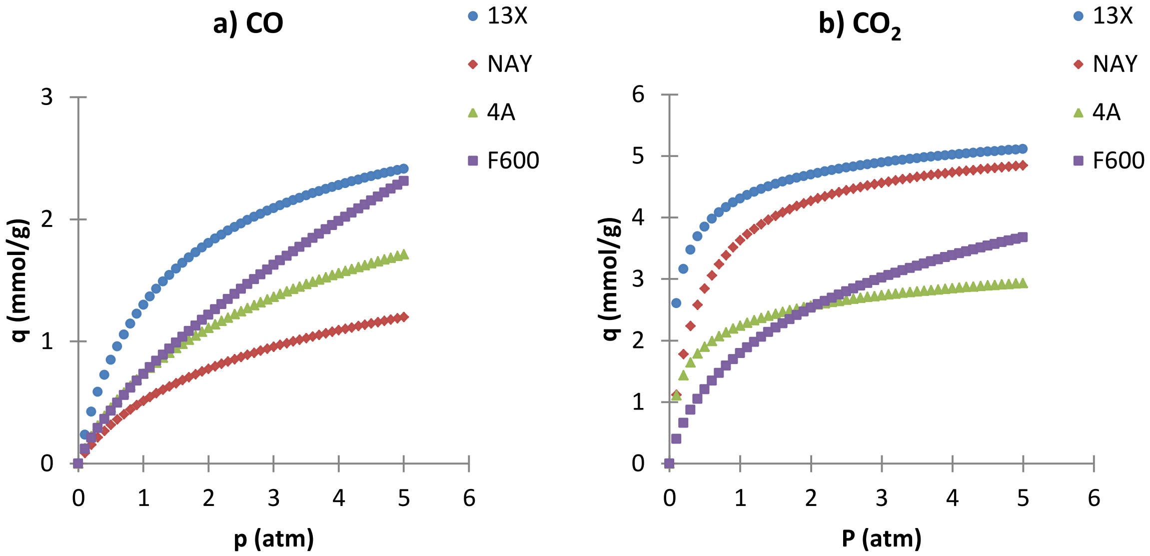

Figure 3: Comparison of adsorption isotherms with different adsorbents studied for a) CO, b) CO_2 at 313K

CO has a small dipole moment. It was reported in literature (Sethia et al., 2010; Tsyganenko et al., 1999; Chowdhury et al., 2012) that there is electrostatic interaction between CO molecules and zeolite extra-framework. Ratio of the SiO_2/Al_2O_3 has an important role for CO adsorption, due to strong interaction of CO with Na+ cation. By decreasing SiO_2/Al_2O_3 ratio in the zeolite structure, the number of Na+ cations per unit cell increases. Therefore, more CO molecules can be adsorbed on the zeolite. The C-O bond could interact with Na+ cations in zeolites, as well as dispersion forces. At low loadings, CO adsorption capacity is high; however, as the cation centres are occupied by

CO molecules, electrostatic interactions are reduced and adsorption will be decreased. Similar to CO_2 case, adsorption of CO on the zeolite 13X is more than on zeolite NaY due to its lower SiO_2/Al_2O_3 ratio. It was reported that CO adsorption at high temperature decreases less than CO_2 adsorption at high temperatures (Xie et al., 1996). Figure 4 shows desorption results for CO and CO_2 from zeolite 13X and zeolite NaY at 313K, as well as the adsorption results. From this figure one can observe that both components have shown good desorption at this temperature, which is in good agreement with adsorption data. For CO data, adsorption from zeolite NaY has shown slightly better reversibility than 13X. Desorption at higher temperatures were also carried out for both adsorbents, which resulted in excellent adsorption reversibility for CO_2, but low reversibility for CO at higher temperatures (373K). The temperature of the PSA must be kept low because of that. Otherwise, PSA columns would be difficult to regenerate and efficiency of system would be decreased. CO may be chemisorbed at higher temperatures.

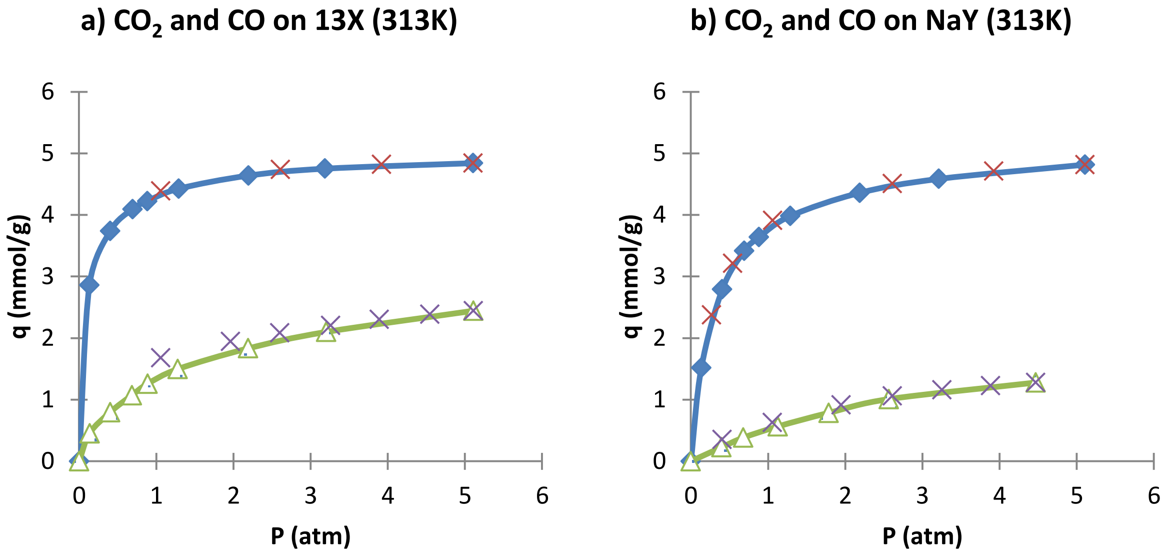

Figure 4: Adsorption and desorption of CO_2 and CO a) zeolite 13X b) zeolite NaY: (×) desorption, (♦) CO_2 adsorption, (Δ) CO adsorption

5.2. Henry's law constant and isosteric heat of adsorption

At the region of Henry's law, the shape of adsorption isotherm curves is dependent on K_p (Henry's Law Constant) values. Higher K_p values indicate steeper and therefore a more rectangular curve which can be observed at low fractional loading. Table 7 shows Henry's law constants determined for different adsorbents studied based on the Toth isotherm model.

Table 7: Henry's law constants for CO_2 and CO adsorption on selected adsorbents studied.

Adsorbate	Henry's law constant, K_p (mmol/g/atm)			
	Zeolite 13X	**Zeolite NaY**	**Zeolite 4A**	**AC F-600**
CO_2	42.16	15.20	13.25	2.61
CO	2.49	0.83	1.01	0.99

Since zeolite 13X has higher K_p values, the initial adsorption of 13X is strong and desorption could be more challenging. Therefore a high vacuum will be required to desorb $CO_{2.}$ This issue must be considered in industrial applications where creating high vacuum could be expensive.

Figure 5 presents the isosteric heat of adsorption for CO_2 and CO gases for the adsorbents studied. Because of the lowest SiO_2/Al_2O_3 ratio, 4A zeolite has shown the highest isosteric heat of adsorption for CO_2 at higher loading. This could be due to the quadrupole interaction of the cationic surface of the adsorbent with CO_2 molecule (Huang, 1973). This isosteric heat on zeolite 4A is less than for the other adsorbents at lower loadings but increases dramatically by increasing adsorption loading. This indicates that adsorbate-adsorbate interactions dominate as loading increases. The isosteric heat for CO_2 adsorption on zeolite 13X is the highest at lower loading and then it decreases slightly by increasing loading. The isosteric heat of CO_2 adsorption on zeolite NaY doesn’t change significantly with changing the CO_2 loading. A consistent isosteric heat during adsorption process indicates lower heterogeneity for the adsorbent zeolite NaY, which is consistent with higher SiO_2/Al_2O_3 ratio for this adsorbent (See Table 3). The decrease in isosteric heat with increasing loading for AC F-600 is more than that for zeolite 13X due to weakening of interactions between adsorbate and the adsorbent.

As shown in Figure 5b, the isosteric heat for CO adsorption for activated carbon showed the highest isosteric heat at low loadings. For CO adsorption, similar to CO_2 adsorption, there is no significant change in the isosteric heat value for zeolite NaY with increasing loading. CO isosteric heat for zeolite 4A and activated carbon F-600 are more than those for 13X and NaY. For both zeolite 13X and NaY, the isosteric heat for CO_2 is higher than for CO, unlike the F-600 activated carbon whose isosteric heat for CO is more than that for CO_2. From these figures it is possible to predict that zeolite NaY has suitable isosteric heat for CO_2/CO separation comparing to 13X. zeolite NaY has slightly less isosteric heat for CO_2 and on the other side isosteric heat of adsorption for CO on zeolite 13X will decreases resulting to better CO adsorption at higher loading.

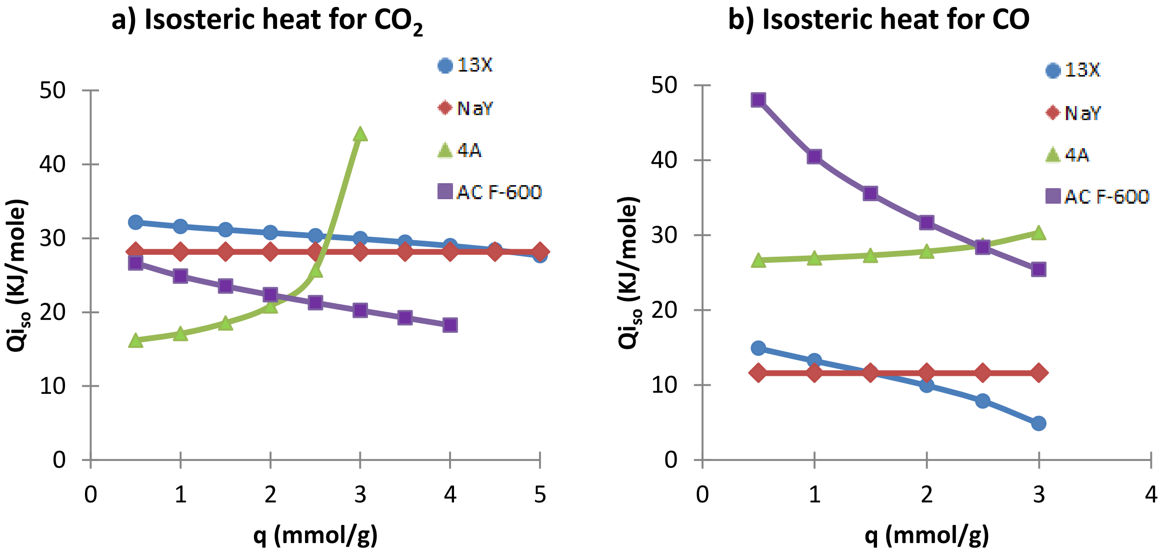

Figure 5: Isosteric heat of adsorption values for CO_2 and CO for Zeolites 13X, NaY, 4A, and Activated Carbon F-600.

5.3. Ideal Selectivity from Pure Component Data

Figure 6 illustrates CO_2/CO variation of ideal selectivity for each selected adsorbents based on Toth model at 313K. This temperature was chosen due to process conditions downstream of RWGS reactor. This selectivity has been calculated by dividing the amount of the pure CO_2 adsorbed over the amount of CO adsorbed (q_{co^2}/q_{co}) at the same pressure for different adsorbents. As shown in this figure zeolite NaY has the highest ideal selectivity. However, selectivity decreases by increasing the pressure confirming that PSA must be designed to operate at lower pressures.

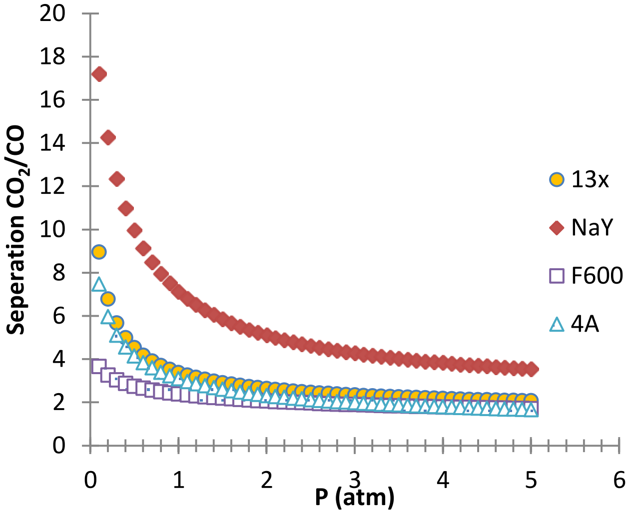

Figure 6: Comparison of separation factors for CO_2 and CO calculated from pure adsorption isotherms for adsorbents studied at 313K.

5.4. Multicomponent Mixture Isotherms

Parameters of the Langmuir isotherms determined from the pure gas data were used according to equation (10) in Section 4.3, in order to predict the ternary adsorption of CO_2, CO and H_2, after the RWGS reactor after the removal of moisture. In this prediction it has been assumed that H_2 will pass through the adsorption column without being adsorbed. Also the maximum mole fraction of CO_2 in the feed stream before reactor is 0.5 since feed contains both CO_2 and H_2 at the same mole fraction. Figure 7 presents these predictions of CO_2 and CO adsorption in ternary mixture (downstream of RWGS reactor) for 4 adsorbents studied.

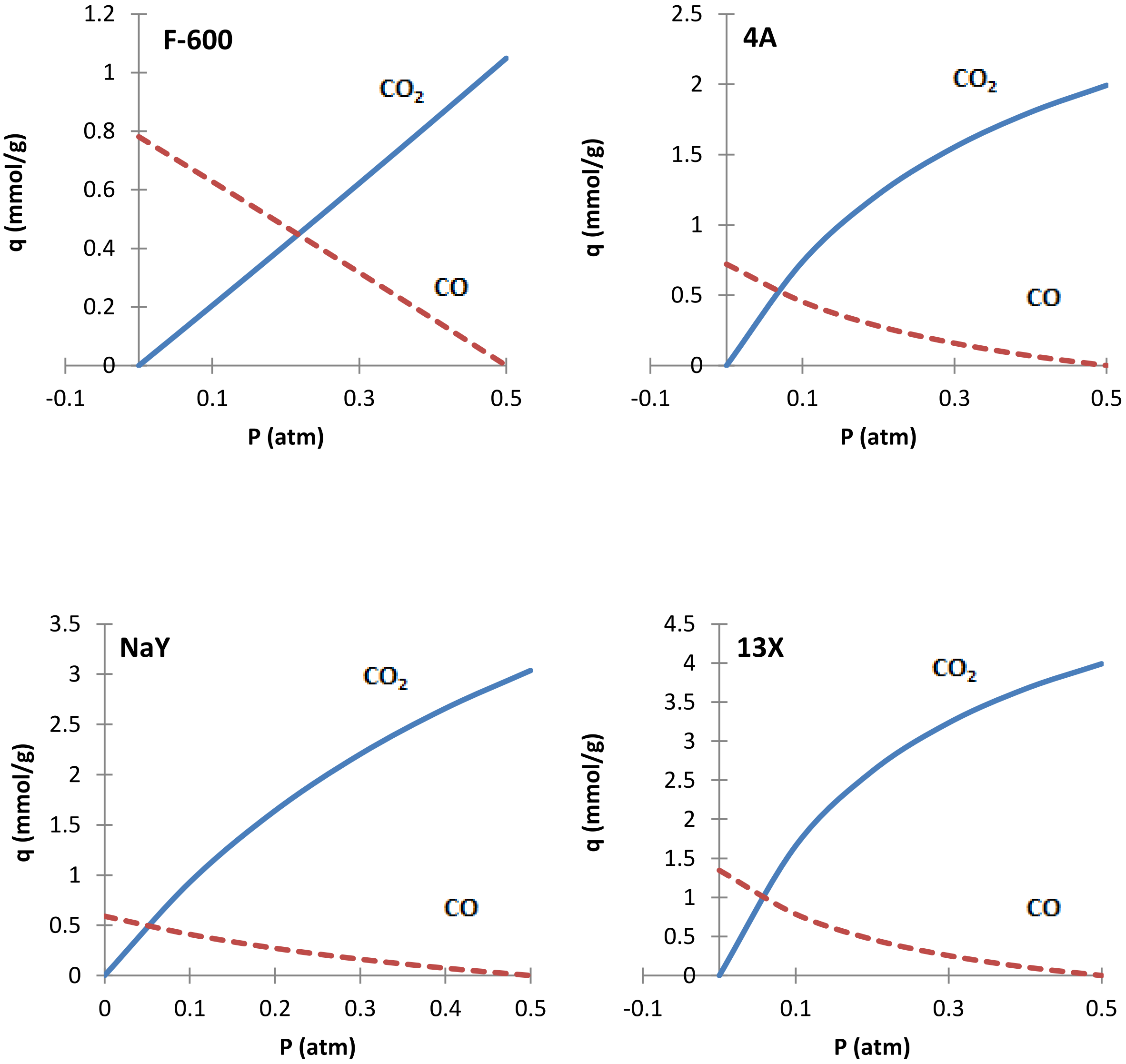

Figure 7: Prediction of CO_2 and CO adsorption in ternary mixture for a total pressure of 1 atm at 313K, for the 4 adsorbents studied: (- - -) CO, (—) CO_2

5.5. Selectivity from Multicomponent Predictions

From ternary mixture predictions, selectivity for each adsorbent can be calculated according to Equation (11). Table 8 shows selectivity factors for investigated adsorbents at 313K. As shown in this table, zeolite NaY has the highest selectivity among the screened adsorbents. However, zeolite 13X could be also a suitable candidate for further studies in real multicomponent adsorption separation, since its selectivity is close to the one for NaY.

Table 8: Selectivity factors CO_2/CO for tested adsorbents at 313 K.

Adsorbent	Zeolite 13X	Zeolite NaY	Zeolite 4A	AC F-600
Selectivity	16.93	18.12	13.03	2.61

5.6. Expected working capacity

The expected working capacities (EWC) for TSA cycles for different blow-down temperatures was estimated based on the Temperature-Dependent Toth isotherm model for CO_2 as feed at 313K at 1 atm pressure and blow-down pressure of 1 atm. These values are shown in Figure 8 for the four adsorbents looked at in this study. As shown in this figure, by increasing the temperature of the blow-down step, the working capacity increases, as expected, since adsorption capacity decreases as temperature increases. However this increase in EWC dramatically diminishes above a certain temperature for each adsorbent indicating that it would not be economically feasible to increase regeneration temperature further. As shown in Figure 8, working capacities for zeolite 13X and NaY are higher than those for zeolite 4A and AC F-600. Also zeolite NaY could achieve the highest working capacity among the adsorbents at blow-down step with a regeneration temperature less than 523K which shows its good potential as an adsorbent for the TSA system.

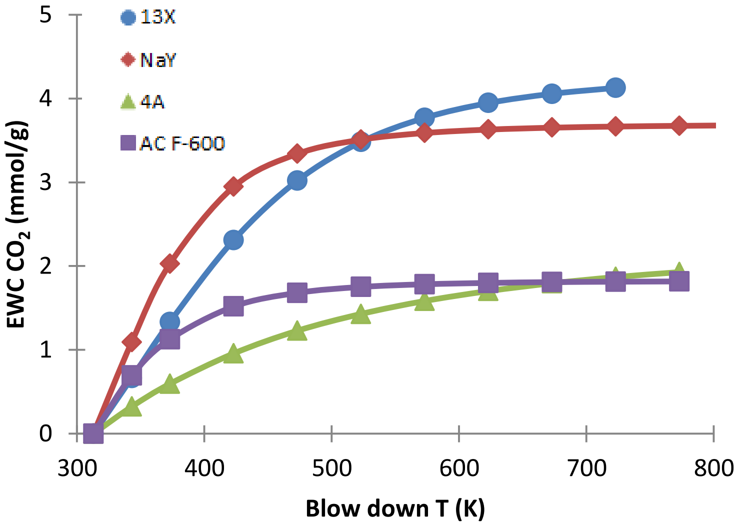

Figure 8: Comparison of expected working capacities for a feed of CO_2 at 313K, 1 atm as a function of blow down temperature at 1 atm, for TSA application.

Figure 9 illustrates expected working capacities for zeolites NaY and 13X for PSA and PTSA cycles, calculated from Equation (12), for different regeneration pressures. For the

PSA cycles, the feed is considered pure CO_2 at 1 atm and at different temperatures (313K, 343K and 373K). For the blow-down cycle was considered at different vacuum pressures and at the same temperature as the feed (313K, 343K and 373K). In the case of PTSA cycles feed is considered pure CO_2 at 313K and 1 atm while blow down cycle was considered at different vacuum pressures and raised temperature of 373K.

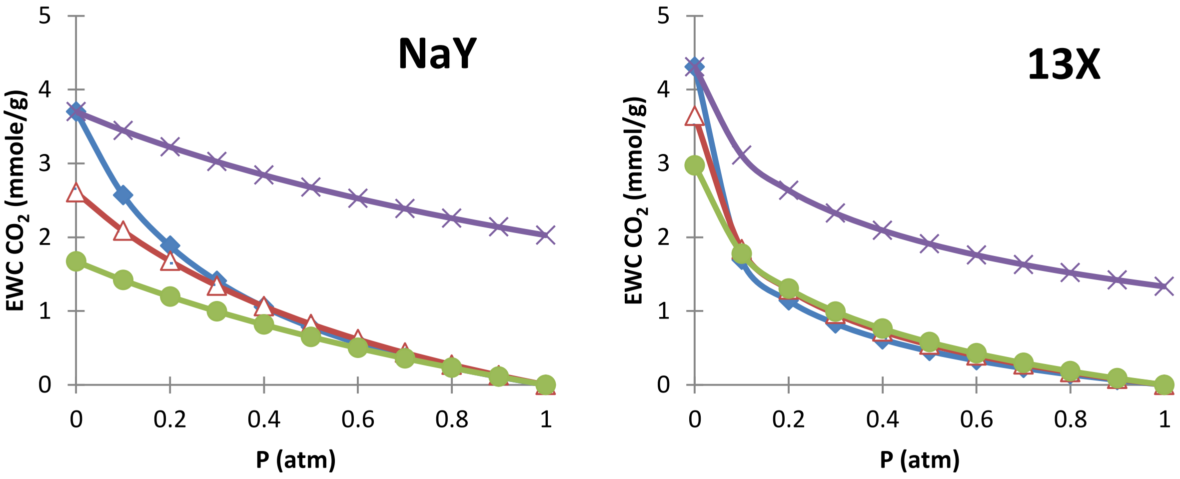

Figure 9: EWC for zeolites NaY and 13X; PSA cycles for a feed of CO_2 at 1 atm and (♦) 313K, (Δ) 343K and (•) 373K and blow-down cycles at different vacuum pressures at the same temperatures; PTSA cycles for a feed of CO_2 at 1 atm and 313K and blow down cycles at different vacuum pressures at 373K (×).

As could be observed in this figure, PTSA can provide more expected working capacity for CO_2 separation by adsorption. Also in the case of zeolite NaY, working capacity in a PTSA system is less sensitive to vacuum pressure compared to zeolite 13X. For PSA, the temperature of feeding steps has a significant effect on the working capacity if a very high vacuum could be provided for blow-down steps for zeolite NaY. As shown in this figure, for blow-down pressures higher than 0.1 atm, there is no significant difference between expected working capacities for different feed temperatures when 13X is used as the adsorbent. Therefore for a PSA system, suitable vacuum is needed regardless of adsorption temperature. Since maintaining high vacuum is expensive, especially in large industrial scales, TSA with zeolite NaY can be an efficient method for CO_2/CO separation downstream of RWGS reactor.

6. Conclusions

For all the adsorbents studied and at all temperatures, the amount of CO_2 adsorbed is much higher than CO as could be predicted, due to smaller molecular size of CO_2, its polarizibility and acidity. Both Langmuir and Toth isotherm models are fitted with experimental data. However, the Toth isotherm model has shown more validity than Langmuir isotherm model especially at higher pressures for CO adsorption, for the adsorbents studied. Selectivity factor for these gases decreases with increasing pressure and it was the highest for zeolite NaY among all of the adsorbents. Isosteric heat of CO adsorption by zeolite 13X and NaY don't change significantly with adsorption loading. However, zeolite 4A has shown a sharp increase in isosteric heat of CO_2 adsorption at higher loading. Also the isosteric heat of adsorption for CO on zeolite 13X decreased with increasing loading resulting in better CO adsorption. Among tested commercial adsorbents, zeolite NaY has shown the best separation ability for CO_2 and CO at pressures up to 5 atm due to its selectivity and isosteric heat of adsorption comparing to zeolite 13X. In addition, the working capacity of NaY for a TSA process was determined to be the highest among the investigated adsorbents.

7. References

Abdollahi, F., F.H. Tezel, and S. Aplin, (2012). “Increasing conversion of CO_2 to CO via RWGS reaction: simulation and process design”, submitted to Alternative Energy.

Ahn, H., J. H. Moon, S. H. Hyun and C. H. Lee (2004). "Diffusion mechanism of carbon dioxide in zeolite 4A and CaX pellets." Adsorption-Journal of the International Adsorption Society **10**(2): 111-128.

Beck, D. W. (1974). Zeolite Molecular SieVes; Wiley & Sons: New York

Berlier, K. and M. Frere (1996). "Adsorption of CO_2 on activated carbon: Simultaneous determination of integral heat and isotherm of adsorption." Journal of Chemical and Engineering Data **41**(5): 1144-1148.

Cai W.Q., T. E. Gough, X. J. Gu, N. R. Isenor, and G. Scoles (1987). "Polarizability of CO_2 studied in molecular-beam laser Stark spectroscopy". Phys. Rev. A **36**, 4722–4727

Cavenati, S., C. A. Grande and A. E. Rodrigues (2004). "Adsorption equilibrium of methane, carbon dioxide, and nitrogen on zeolite 13X at high pressures." Journal of Chemical and Engineering Data **49**(4): 1095-1101.

Chetty N. and V.W. Couling (2011). "Measurement of the electric quadrupole moment of CO." J Chem Phys. **134**(16):164307

Chowdhury, P., S. Mekala, F. Dreisbach and S. Gumma (2012). "Adsorption of CO, CO_2 and CH4 on Cu-BTC and MIL-101 metal organic frameworks: Effect of open metal sites and adsorbate polarity." Microporous and Mesoporous Materials **152**: 246-252.

Chue, K. T., J. N. Kim, Y. J. Yoo, S. H. Cho and R. T. Yang (1995). "Comparison of activated carbon and zeolite 13x for CO_2 recovery from flue-gas by pressure swing adsorption." Industrial & Engineering Chemistry Research **34**(2): 591-598.

Doty, F. D., G. N. Doty, J. P. Staab and L. L. Holte (2010). "Toward efficient reduction of CO_2 to CO for renewable fuels." Es2010: Proceedings of Asme 4th International Conference on Energy Sustainability, **1**: 775-784.

Harries J.E. (1970). "The quadrupole moment of CO_2, measured from the far infrared spectrum." J. Phys. B: At. Mol. Phys. **3** L150

Harlick, P. J. E. and F. H. Tezel (2002). "Adsorption of carbon dioxide, methane, and nitrogen: Pure and binary mixture adsorption by ZSM-5 with SiO_2/Al_2O_3 ratio of 30." Separation Science and Technology **37**(1): 33-60.

Harlick, P. J. E. and F. H. Tezel (2004). "An experimental adsorbent screening study for CO_2 removal from N_2." Microporous and Mesoporous Materials **76**(1-3): 71-79.

Huang, Y. Y. (1973). "Quadrupole interaction of Carbon-Dioxide on Silica-Alumina surface." Journal of Physical Chemistry **77**(1): 103-106.

Kikkinides, E. S., R. T. Yang and S. H. Cho (1993). "Concentration and recovery of CO_2 from flue-gas by pressure swing adsorption." Industrial & Engineering Chemistry Research **32**(11): 2714-2720.

Ko, D., R. Siriwardane and L. T. Biegler (2003). "Optimization of a pressure-swing adsorption process using zeolite 13X for CO_2 sequestration." Industrial & Engineering Chemistry Research **42**(2): 339-348.

Lee, J. S., J. H. Kim, J. T. Kim, J. K. Suh, J. M. Lee and C. H. Lee (2002). "Adsorption equilibria of CO_2 on zeolite 13X and zeolite X/Activated carbon composite." Journal of Chemical and Engineering Data **47**(5): 1237-1242.

Ma, J. H., L. Li, J. Ren and R. F. Li (2010). "CO adsorption on activated carbon-supported Cu-based adsorbent prepared by a facile route." Separation and Purification Technology **76**(1): 89-93.

Maurin, G., P. L. Llewellyn and R. G. Bell (2005). "Adsorption mechanism of carbon dioxide in faujasites: Grand canonical Monte Carlo simulations and microcalorhnetry measurements." Journal of Physical Chemistry B **109**(33): 16084-16091.

Merel, J., M. Clausse and F. Meunier (2008). "Experimental investigation on CO_2 post-combustion capture by indirect thermal swing adsorption using 13X and 5A zeolites." Industrial & Engineering Chemistry Research **47**(1): 209-215.

Mulgundmath, V. P., F. H. Tezel, T. Saatcioglu and T. C. Golden (2012). "Adsorption and separation of CO_2/N_2 and CO_2/CH_4 by 13X zeolite." Canadian Journal of Chemical Engineering **90**(3): 730-738.

Pakseresht, S., M. Kazemeini and M. M. Akbarnejad (2002). "Equilibrium isotherms for CO, CO_2, CH_4 and C_2H_4 on the 5A molecular sieve by a simple volumetric apparatus." Separation and Purification Technology **28**(1): 53-60.

Saha, D. and S. G. Deng (2009). "Adsorption equilibria and kinetics of carbon monoxide on zeolite 5A, 13X, MOF-5, and MOF-177." Journal of Chemical and Engineering Data **54**(8): 2245-2250.

Sayari, A., Y. Belmabkhout and R. Serna-Guerrero (2011). "Flue gas treatment via CO_2 adsorption." Chemical Engineering Journal **171**(3): 760-774.

Scuseria G.E., M.D. Miller, F. Jensen, J. Geertsen (1991). "The dipole moment of carbon monoxide. " Journal of Chemical Physics; Vol. 94 Issue 10, p6660

Sethia, G., G. P. Dangi, A. L. Jetwani, R. S. Somani, H. C. Bajaj and R. V. Jasra (2010). "Equilibrium and dynamic adsorption of carbon monoxide and nitrogen on ZSM-5 with different SiO_2/Al_2O_3 Ratio." Separation Science and Technology **45**(3): 413-420.

Shao, W., L. Z. Zhang, L. X. Li and R. L. Lee (2009). "Adsorption of CO_2 and N_2 on synthesized NaY zeolite at high temperatures." Adsorption-Journal of the International Adsorption Society **15**(5-6): 497-505.

Toth, J. (1995). "Uniform interpretation of gas-solid adsorption." Advances in Colloid and Interface Science **55**: 1-239.

Tsyganenko A.A., E.E. Platero, C.O. Arean, E. Garrone, A. Zecchina (1999). "Variable-temperature IR spectroscopic studies of CO adsorbed on Na-ZSM-5 and Na-Y zeolites. " Catalysis Letters **61**: 187-192.

Walton, K.S. and M. D. LeVan (2006). "A novel adsorption cycle for CO_2 recovery: Experimental and theoretical investigations of a temperature swing compression process." Separation Science and Technology **41**(3): 485-500.

Wirawan S.K. and D. Creaser (2006 a) "CO_2 adsorption on silicalite-1 and cation exchanged ZSM-5 zeolites using a step change response method." Microporous and Mesoporous Materials **91**: 196-205.

Wirawan S.K. and D. Creaser (2006 b). "Multicomponent $H_2/CO/CO_2$ adsorption on BaZSM-5 zeolite. " Separation and Purification Technology **20**; 52: 224-231.

Xie Y.C., J.P. Zhang, J.G. Qiu, X.Z. Tong, J.P. Fu, G. Yang, H. Yan, Y. Tang (1996). "Zeolites modified by CuCl for separating CO from gas mixtures containing CO_2". Adsorption-Journal of the International Adsorption Society **3**: 27-32.

Zhang, J., P. A. Webley and P. Xiao (2008). "Effect of process parameters on power requirements of vacuum swing adsorption technology for CO_2 capture from flue gas." Energy Conversion and Management **49**(2): 346-356.

Chapter IV: Breakthrough adsorption experiments for CO_2/CO on zeolite NaY and 13X

Farhang Abdollahi(1), F. Handan Tezel(1), Stephen Aplin(2)

(1) University of Ottawa, Department of Chemical and Biological Engineering, Ottawa, ON, Canada

(2) The HDP Group, Ottawa, ON, Canada

Keywords: Alternative energy, CO_2 conversion, Synthetic fuel, Reverse water gas shift reaction (RWGS)

Abstract

Converting CO_2 to CO through Reverse Water Gas Shift (RWGS) reaction can reduce CO_2 emission from coal power plants and produce valuable active CO. In order to increase CO_2 conversion to CO, separation of these gases downstream of RWGS reactor was studied by means of adsorption process in order to recycle back unreacted CO_2 to the RWGS reactor inlet. In our previous study, an adsorbent screening had been carried out and zeolite NaY was determined as the most suitable adsorbent for this process. Adsorption columns packed with zeolites NaY and 13X were used in order to ensure their performance for real multicomponent (CO_2/CO/H_2) mixture that resembles the RWGS reactor outlet. Breakthroughs for each component in both dry and water saturated conditions were obtained by means of lab scale adsorption set up in this study. The outlet of the adsorption column was connected to a gas chromatograph (GC) and concentration of each component was measured as a function of time in order to evaluate adsorbent performance. Blow down (desorption) and second cycle adsorption after blow down of

the column were carried out here to study the suitability of the adsorption system under repeated adsorption/desorption cycles. Adsorption process with zeolite NaY has shown promise for the separation of CO_2 from CO with high purity and recovery at low pressure and at ambient temperature.

1. Introduction

Importance of more investigation on alternative energy sources has increased recently, due to increasing green-house gas (GHG) emission and its effect on global warming, as well as due to depletion of natural resources, especially fossil fuels. Reducing CO_2 emission by capturing from flue gas could be an important step in order to minimize GHG emission, but it would not be sufficient. Conversion of captured CO_2 to valuable products could justify value of carbon capture and sequestration (CCS) plants. CO_2 can be converted to CO which is a very active precursor to produce a wide range of valuable products such as alcohol, acids and synthetic fuels. This conversion can be achieved through Reverse Water Gas Shift (RWGS) reaction during which CO_2 reacts with H_2 to produce CO and water. Since RWGS reaction is an endothermic reversible reaction, only a portion of CO_2 will be converted to CO. Therefore unreacted CO_2 must be recycled back into the RWGS reactor in order to maximize CO_2 conversion. However, downstream of RWGS reactor contains CO_2, CO, H_2 and water. Hence, a separation system is required to separate CO_2 from CO and H_2 after the removal of water. For post RWGS process, H_2, together with CO could be sent to another reactor to produce combustible hydrocarbons such as a Fischer-Tropsch reactor or a methanol production unit.

Adsorption processes are one of the most cost effective and efficient processes for separation of gases (Cavenati et al., 2006; Grande & Rodrigues, 2008; Zhang et al., 2008). There are different process concepts in the field of adsorption such as Pressure Swing Adsorption (PSA), Vacuum swing adsorption (VSA), Temperature Swing Adsorption (TSA) and Pressure Temperature Swing Adsorption (PTSA). VSA is an expensive option for big industrial scale due to expensive vacuum pumps and operation. For this project PSA and TSA have been considered as potential separation systems downstream of the RWGS reactor.

Adsorption separation of CO_2 from different streams such as from flue gas and natural gas was investigated in many studies in the literature, however adsorption selectivity of CO_2/CO needs to be studied further in order to determine the best operating conditions for this separation. In our previous studies, adsorbent screening was carried out by looking at heat of adsorption, Henry's law constants and selectivity factors for CO_2 and CO to determine the best adsorbent to separate unreacted CO_2 at the outlet of the RWGS reactor from a stream containing CO and H_2 after the removal of water. Zeolite NaY has been considered as an efficient adsorbent candidate for a TSA process (Abdollahi, et al., 2012).

In this study, a real multicomponent mixture of gases downstream of the RWGS reactor was sent through a packed adsorption column and adsorption capacity for CO_2/CO/H_2 separation as well as breakthrough curves at various operating conditions and feed concentrations were determined. Desorption of all adsorbed gases were studied in order to determine the working capacity of the adsorbent. Selectivity factors have been calculated and then CO_2 breakthrough curves in different conditions were modeled.

2. Experimental:

Figure 1 shows the schematic diagram of the lab set up used for adsorption system. Upstream of system contains 3 gas cylinders for CO_2, CO and H_2 with 99.9 (wt.%) purity obtained from Linde Canada (Burlington, Ontario, Canada). Each gas cylinder has been connected to mass flow controllers (MFC's) obtained from MKS (Andover, Massachusetts, USA) with maximum range of 100 ml/min. Precision of these MFC's is 1.5 % of their maximum range. These MFC's have been use to control the composition of the multicomponent mixture going into mixer and then into the adsorption column. In order to study the effect of saturated water in the gas stream on the adsorption of CO_2 and CO, one Erlenmeyer flask (bubbler) was installed before adsorption column to saturate the gas mixture with water. This bubbler could be by-passed in the case of the dry stream going into the adsorption column. The column (22cm ID and 33 cm in length) was considered adiabatic since it was wrapped in heating tape and an isolator of fiber glass with a refractory material. The characteristics of the adsorption column are presented in Table 1. A by-pass tube was installed around the column for determining the composition of the inlet gas mixture prior to the adsorption process. Also a pressure gauge was installed at the inlet of the column to record pressure changes. Two thermocouples were connected to the inlet and outlet of the column to measure temperature changes with time. Both inlet and outlet compositions for the adsorption column were analyzed by a gas chromatograph (GC) built by GOW-MAC series 580 (Bethlehem, Pennsylvania, USA) equipped with a thermal conductivity detector (TCD, WX7) and a Porapak Q column. A Thermo scientific Vacuum pump was installed at downstream of GC in order to regenerate and degas the adsorbent. All piping was provided from Swagelok (Ottawa, ON, Canada). GC operation temperatures were 50°C, 85°C and 62°C for column, detector and injection, respectively.

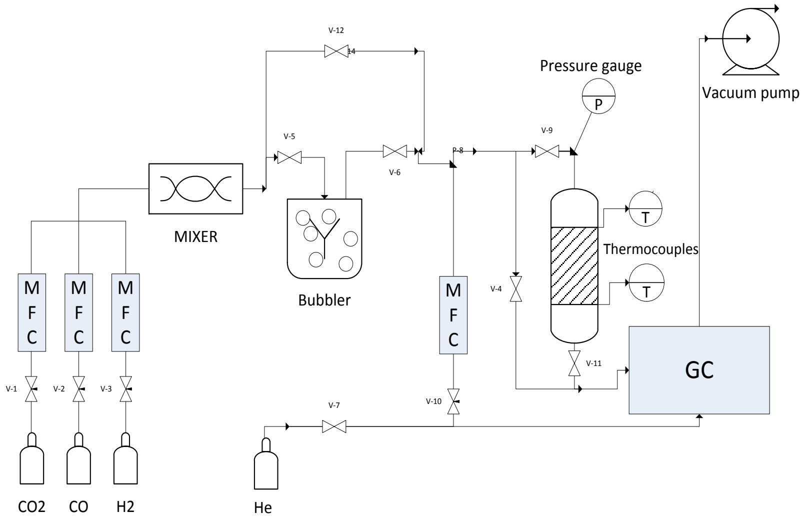

Figure 1: Schematic diagram of the lab set up used for multi component adsorption breakthrough. MFC: Mass Flow Controller, GC: Gas Chromatograph

Table 1: Characteristics of the adsorption column used for breakthrough curves.

L (length of the adsorption column)	32.5 cm
ID (inner diameter)	2.1 cm
V (volume of the adsorption column)	112.6 cm^3
ε (void fraction)	0.4
τ (contact time)= ε×V/ flow rate	10 – 12.85 seconds
Adsorbent Pore radius, rp	8×10^{-8} cm
Adsorbent Particle radius, Rp	0.07 cm
Wall thickness	0.1 cm

Adsorbent was degassed before each experiment at the temperature of 350oC under vacuum for at least 8 hours. Then Helium was passed through adsorption column for an hour to strip any possible component left in the adsorbent and at the end, vacuum pump was applied to purge helium from the column. GC was kept on for at least two hours before measuring compositions to stabilize all temperatures and helium flow rate as GC career gas. Based on the operating conditions inside the RWGS reactor and the corresponding equilibrium CO_2 conversion, different compositions of the gas mixture were prepared using the MFCs and fed into the adsorption column through both bubbler and its bypass. The reason for passing the stream through the bubbler was to saturate the feed gas with moisture, which would resemble the gases coming out from the RWGS reactor after the condenser. The feed composition before the adsorption process was determined by the GC bypassing the adsorption column. Then bypass valve was closed and adsorption process commenced. Outlet of the adsorption column was injected into the GC approximately every 160 seconds to measure its composition. By analyzing the outlet composition as a function of time, breakthrough curve could be determined and finally the adsorption capacity of the packed column could be determined for each gas.

3. Theory:

Adsorption capacity of the adsorbents for each gas in the multicomponent mixture could be determined by analyzing the breakthrough curves. These capacities will give more realistic values for each gas in the presence of the other gases in the mixture, as opposed to the pure component adsorption capacities. The area above the breakthrough curve is related to the amount of adsorbed gas in the adsorbent. This capacity could be calculated using equation 1:

$$AC_i = \frac{w.Q_i}{m_{adsorbent}} \qquad (1)$$

where AC_i, Q_i, $m_{adsorbent}$ and w are adsorption capacity for component i (ml/$g_{adsorbent}$), the volumetric flow rate for component i (ml/min), mass of adsorbent packed in the column (g) and the area above breakthrough curve (min), respectively.

The variable t_i can be defined in equation 2, corresponding to the calculation of the area above the breakthrough curve.

$$w = \int_0^\infty (1 - \frac{c_i}{c_{i0}})\, dt \qquad (2)$$

In this equation, c_i and c_{i0} represent the mole fraction of component i at the inlet and outlet respectively.

Separation factor can be calculated from equation 3. This factor could be useful in order to compare performance of the adsorption process for different flow rates and conditions (Hashi et al., 2010):

$$S_{CO2/CO} = \frac{x_{CO2}/y_{CO2}}{x_{CO}/y_{CO}} \qquad (3)$$

In this equation X_{CO2} and X_{CO} represent the volume fraction of CO_2 and CO in the adsorbed phase, while Y_{CO2} and Y_{CO} indicate volume fraction in the gas phase for CO_2 and CO, respectively.

Two models were applied in this study to predict CO_2 breakthrough curves. These two models were compared with each other for zeolite NaY.

First model is the Rosen model which has following assumptions (Yang, 1997):

- There is no axial dispersion in the column;
- Adsorption isotherm is linear: fluid phase concentration at the surface of the adsorbent is given by: $q = KC$;
- Gas velocity is constant;
- Effective diffusivity is constant.

According to non-equilibrium theory, breakthrough curves could be obtained by following equation:

$$\frac{C_i}{C_{i0}} = 1/2[1 \pm \mathrm{erf}(\frac{\left(\frac{3U}{2V}\right) - 1}{2(\frac{1+5v}{5V})^{1/2}}) \tag{4}$$

Where V, U and v are will be dimensionless bed length parameter, dimensionless contact time parameter and dimensionless film resistance parameter respectively:

$$V = \frac{3D_e KL}{uR_p^2}(\frac{\varepsilon}{1-\varepsilon}) \tag{5}$$

$$U = \frac{2D_e(t - {}^{L}/_{u})}{R_p^2} \tag{6}$$

$$v = \frac{D_e K}{K_f R_p} \tag{7}$$

Second model is an empirical model which can be fitted with experimental data. One of the most important outcomes of conducting an adsorption experiment in the packed column is to determine the kinetic of the adsorption and maximum adsorption capacity of the adsorbent under certain conditions. In order to obtain a suitable model for time-concentration relation from the breakthrough experiments, an empirical equation proposed by Yan et al. has been implemented for breakthrough data (Yan et al., 2001). But this empirical equation has been modified according to its unit dimensions and term (a) in the equation for this study. This non-linear regression model could describe the breakthrough curves of CO_2 in the adsorption column. Following equation represents the modified model (Yan et al., 2001):

$$\frac{C_i}{C_{i0}} = 1 - \frac{1}{1 + [\frac{Q.\mathrm{t}}{b}]^a} \qquad (8)$$

In this equation a is defined as:

$$a = \frac{k_y.C_{i0}.m}{Q} \qquad (9)$$

Compared to the equation used by Yan et al., (2001), in this model a has presented with mass of adsorbent at numerator. Also b will be presented as:

$$b = \frac{C_{i0}}{q_m.m} \qquad (10)$$

where C_i and C_{io} are mole fraction of component i at the inlet and outlet respectively, k_y is the rate constant (ml/min/g), q_m is the maximum capacity of the adsorbent (ml/g), m is the mass of the adsorbent (g), Q is the volumetric flow rate (ml/min) and t is time (min).

In our previous studies, (Abdollahi et al., 2012) adsorbent screening was carried out in order to find the most appropriate one from selected adsorbents for CO_2/CO separation and zeolite NaY was chosen as a suitable adsorbent for real gas mixture adsorption in this study (Abdollahi et al., 2013). Zeolite NaY (UOP, Des Plaines, IL, USA) showed higher selectivity and stable isosteric heat of adsorption compared to other studied adsorbents (13X, 4A and activated carbon F-600).

Pressure drop across the adsorption column has been calculated from the Ergun equation as equation 11.

$$\frac{\Delta P}{L}=\frac{150(1-\varepsilon_c)^2 \nu_g \mu}{\varepsilon_c^3 \phi^2 D_p^2}+\frac{1.75(1-\varepsilon_c) \upsilon_g^2 \rho_g}{\varepsilon_c^3 \, \phi \, D_p} \qquad (11)$$

In this experiment pressure drop across adsorption column was calculated and considered negligible.

4. Results and discussion

4.1. Comparison of zeolites 13X and NaY

In our previous study (Abdollahi et al., 2013), adsorbent screening for CO_2/CO separation was carried out and zeolite NaY was found to be the best adsorbent for the process because of its selectivity and lower isosteric heat of adsorption compared to zeolite 13X. In order to appreciate those results in real situation both zeolites were investigated for their capability of CO_2/CO separation in ternary mixtures in this study. Figure 2 shows the comparison of CO_2, CO and H_2 breakthrough curves and mole fraction at the outlet of adsorption column for both zeolites 13X and NaY as well as temperature changes at the inlet and outlet of the column. Feed was a mixture of CO_2 (90 ml/min), CO (50 ml/min) and H_2 (90 ml/min) measured and controlled by MFCs. This mixture was prepared according to the composition of downstream of RWGS reactor with 40% of CO_2 conversion to CO. At the beginning one can observe that CO is getting adsorbed with CO_2 on zeolite 13X and after almost 9 minutes CO starts to leave the column when in the case of zeolite NaY it was detected at the beginning of the experiment. Furthermore, temperature changes within the column were measured during the adsorption by means of two thermocouples which were placed at the inlet and the outlet of the column. Adsorption was carried out by a downward flow; therefore the temperature at the top of the column increased due to exothermic adsorption and as mass transfer zone (MTZ) moved toward the end of the column, temperature at the outlet of the column started to increase. As shown in Figure 2, zeolite 13X shows higher temperature change indicating higher heat of adsorption compared to zeolite NaY. This difference in heat of adsorption between two adsorbents were predicted and calculated in adsorbent screening study. Isosteric heat of zeolites 13X and NaY were obtained at different concentration by means of the data acquired from adsorption equilibrium isotherm and they are in very good agreement with real mixture breakthrough experiments (Abdollahi et al, 2013).

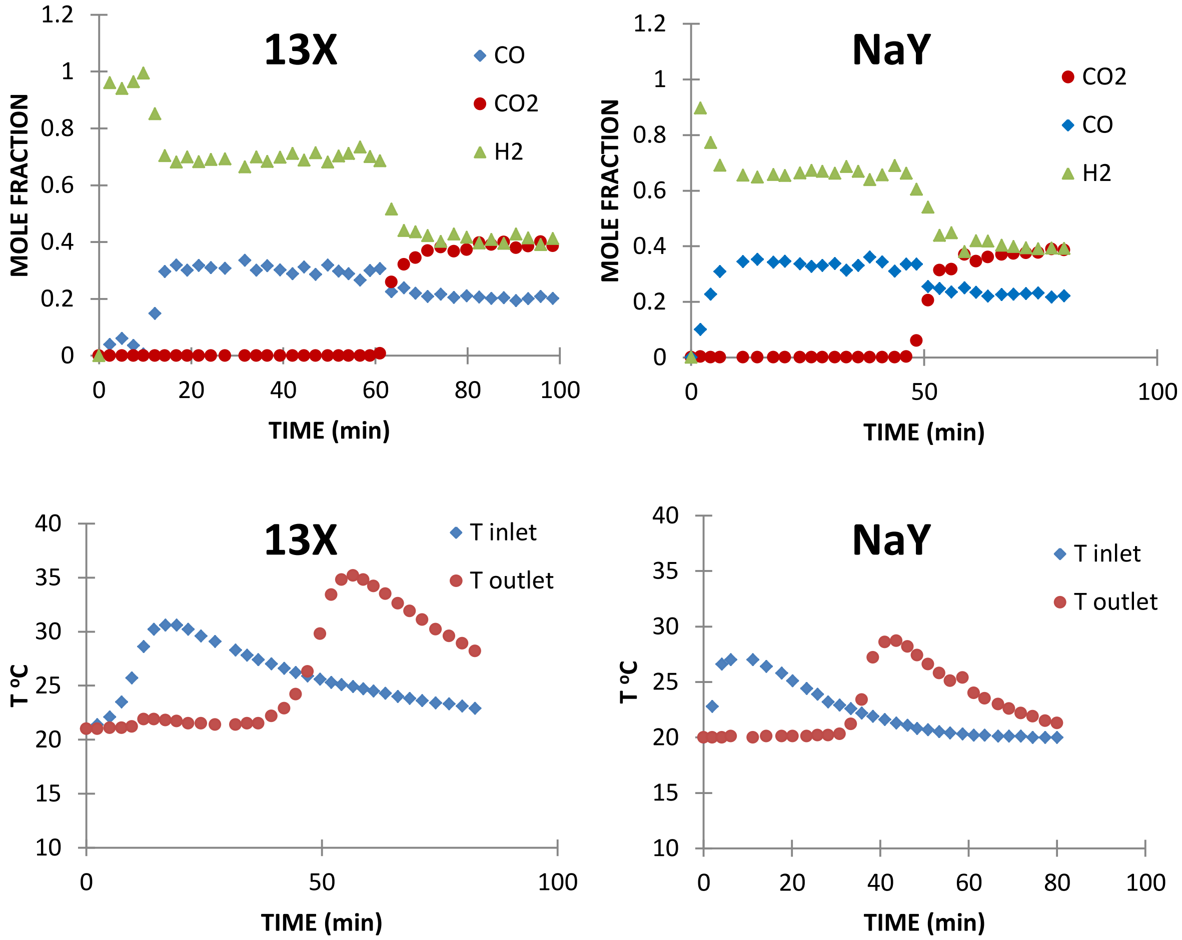

Figure 2: Comparison of zeolite 13X and NaY concentration and temperature breakthrough curves for a mixture of CO_2, CO and H_2 with mole fractions of 0.39, 0.21 and 0.39, respectively at 295K and 1atm total pressure.

Table 2 shows the adsorption capacity and selectivity of zeolites 13X and NaY, calculated from the breakthrough curves in Figure 2, for CO_2 and CO gases. H_2 capacity could not be calculated accurately and assumed to be negligible, since it broke through the column right away. As it could be predicted, zeolite 13X has the higher adsorption capacity for both CO_2 and CO but its selectivity for CO_2/CO separation is much lower compared to zeolite NaY. Also it is less than the predicted selectivity factor for zeolite 13X which was calculated in our previous study (Abdollahi et al, 2013) by using extended Langmuir model for mixtures, which does not take the competitive adsorption into account. In this particular case, the competitive adsorption has been an advantage for the adsorption of CO_2 from the mixture. These results are in agreement with our previous study, as well as other studies in the literature (Walton and LeVan, 2006) that zeolite NaY is a suitable adsorbent for CO_2/CO separation.

Table 2: Adsorption capacity and selectivity factor of zeolite 13X and NaY for a mixture of CO_2 (90 ml/min), CO (50 ml/min) and H_2 (90 ml/min)

Adsorbent	**Weight (g)**	**Cycle**	**Saturated water**	**Feed composition (ml/min) CO_2/CO/H_2**	**CO_2 Breakthrough (min)**	**CO Breakthrough (min)**	**CO_2 Adsorption capacity (ml/g ads)**	**CO Adsorption capacity (ml/g ads)**	**Selectivity**
NaY	64.91	first	no	90/50/90	46	-	72.63	2.34	17.17
13X	73.1	first	no	90/50/90	61	9	78.27	7.97	5.45

4.2. Effect of CO concentration in the feed

In order to study the effect of different compositions at the outlet of RWGS reactor (due to different CO_2 conversions) on the separation process, 3 different mixtures were considered by changing the CO flow rate in the feed. Then these different mixtures were passed through the adsorption column and outlet compositions were studied by GC. Figures 3-5 show the breakthrough curves related to each feed composition. In all figures H_2 immediately starts to come out from the column without being adsorbed, and therefore its adsorption is considered negligible. The same phenomena could be seen about CO with a lower slope for its breakthrough curve indicating that very small amount of CO was adsorbed at the beginning and in a very short time it reached to its initial composition. These results prove that CO and CO_2 could be separated efficiently by means of zeolite NaY. Table 3 compares the breakthrough times and selectivity for different feed compositions.

Table 3: Comparison of adsorption capacity and selectivity factors for different feed compositions.

Adsorbent	**Weight (g)**	**Cycle**	**Saturated water**	**Feed composition (ml/min) $CO_2/CO/H_2$**	**CO_2 Breakthrough (min)**	**CO Breakthrough (min)**	**CO_2 Adsorption capacity (ml/g)**	**CO Adsorption capacity (ml/g)**	**Selectivity**
NaY	68.44	first	no	90/90/90	61	-	85.64	5.47	15.63
NaY	64.91	first	no	90/50/90	46	-	72.63	2.34	17.17
NaY	66.48	first	no	90/30/90	45	-	65.28	0.92	23.46

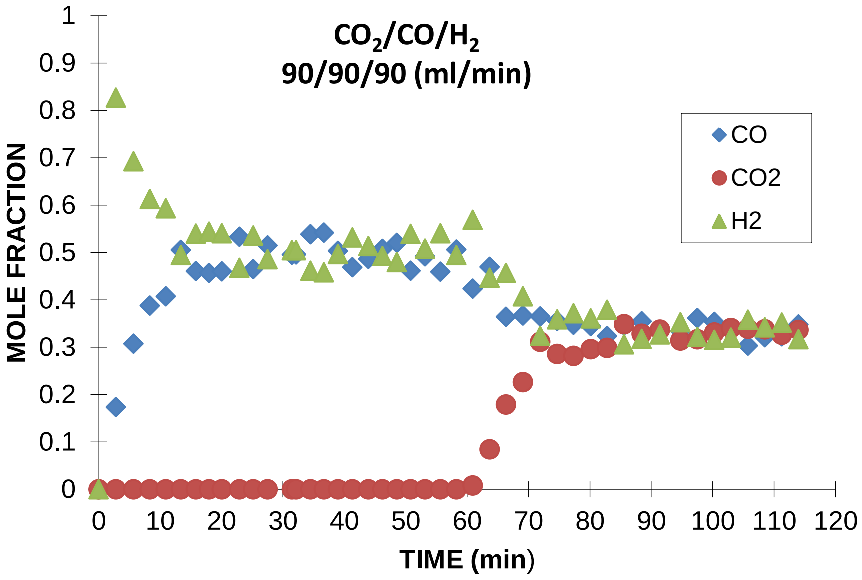

Figure 3: Outlet composition of adsorption column for the feed including 90 ml/min for each gas (CO_2, CO and H_2; 33.3% each) at 295K and 1 atm. Total pressure.

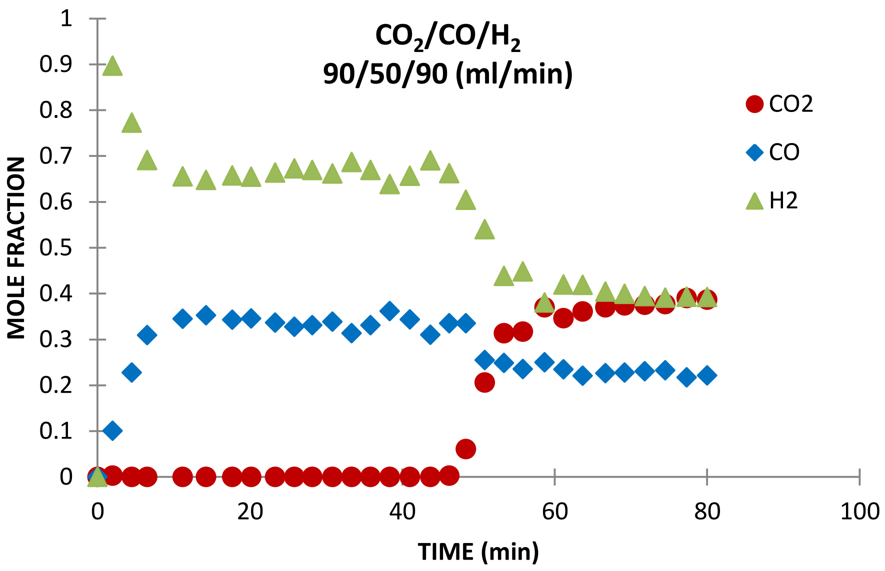

Figure 4: Outlet composition of adsorption column for the feed 90 ml/min CO_2, 50 ml/min CO and 90 ml/min H_2 with a mole fraction of CO_2 (0.43), CO (0.14) and H_2 (0.43) at 295K and 1 atm. total pressure.

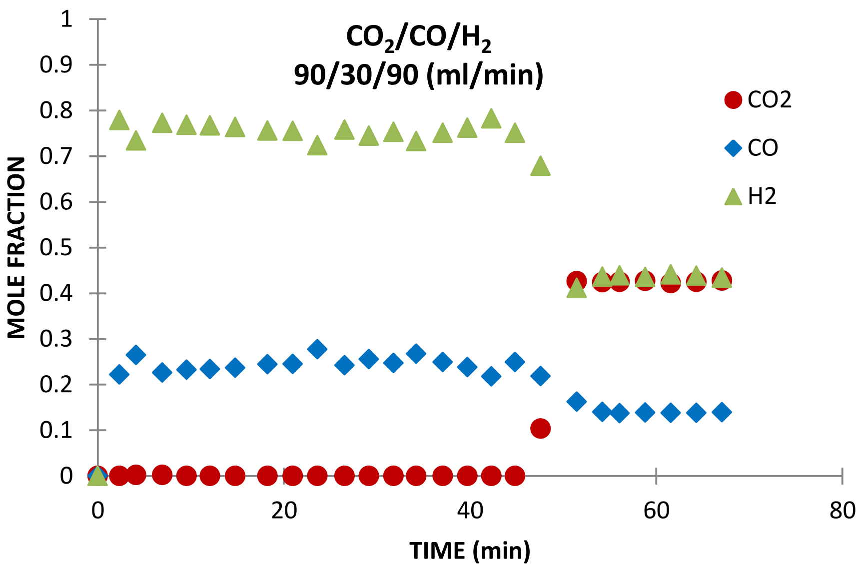

Figure 5: Outlet composition of adsorption column for the feed including 90 ml/min CO_2, 30 ml/min CO and 90 ml/min $H_{2,}$ with a mole fraction of CO_2 (0.43), CO (0.14) and H_2 (0.43) at 295K and 1 atm. total pressure.

It could be interpreted from these results that selectivity factor increases by reducing the volume of CO in the feed indicating that CO_2 could suppress CO adsorption more in competitive adsorption when there is lower mole fraction of CO in the stream, which is expected.

4.3. Working capacity testing by blow down step

In industrial applications, numerous adsorption and desorption cycles are applied to the adsorption packed bed. Difference between the capacities of the column at the end of adsorption and desorption cycles implies working capacity of that column. Two potential modes of operation for adsorption process could be pressure swing adsorption (PSA) and temperature swing adsorption (TSA). For PSA desorption, blow-down step would be carried out by creating a vacuum in the column or decreasing pressure to atmospheric pressure depending on adsorption operation conditions. In the case of TSA, a purge gas could be used at elevated temperature to desorb the adsorbed gases. For CO_2/CO separation downstream of RWGS reactor in industrial scale, it is preferred to avoid high cost of vacuum, since the best separation could take place at lower pressures around atmospheric. Therefore TSA was considered in order to investigate desorption and re-feeding cycle for this study. Since the H_2 should be mixed with CO_2 at the inlet of RWGS reactor, it is the best option for stripping adsorbed CO_2 in the column. Therefore, for desorption cycle, H_2 was used as a purge gas at 373K at a flow rate of 30 ml/min to strip CO_2 from the bed. Higher working capacity can be achieved at higher regeneration temperatures but an economic analysis for project must be performed to determine the optimized desorption temperature and flow rate in industrial scale. For a feed mixture of

CO_2 (90 ml/min), CO (50ml/min) and H_2 (90 ml/min), Figure 6 illustrates a) first adsorption cycle, b) desorption (blow down step) with H_2 as purge gas at 30 ml/min and 373K and c) another adsorption cycle after blow-down.

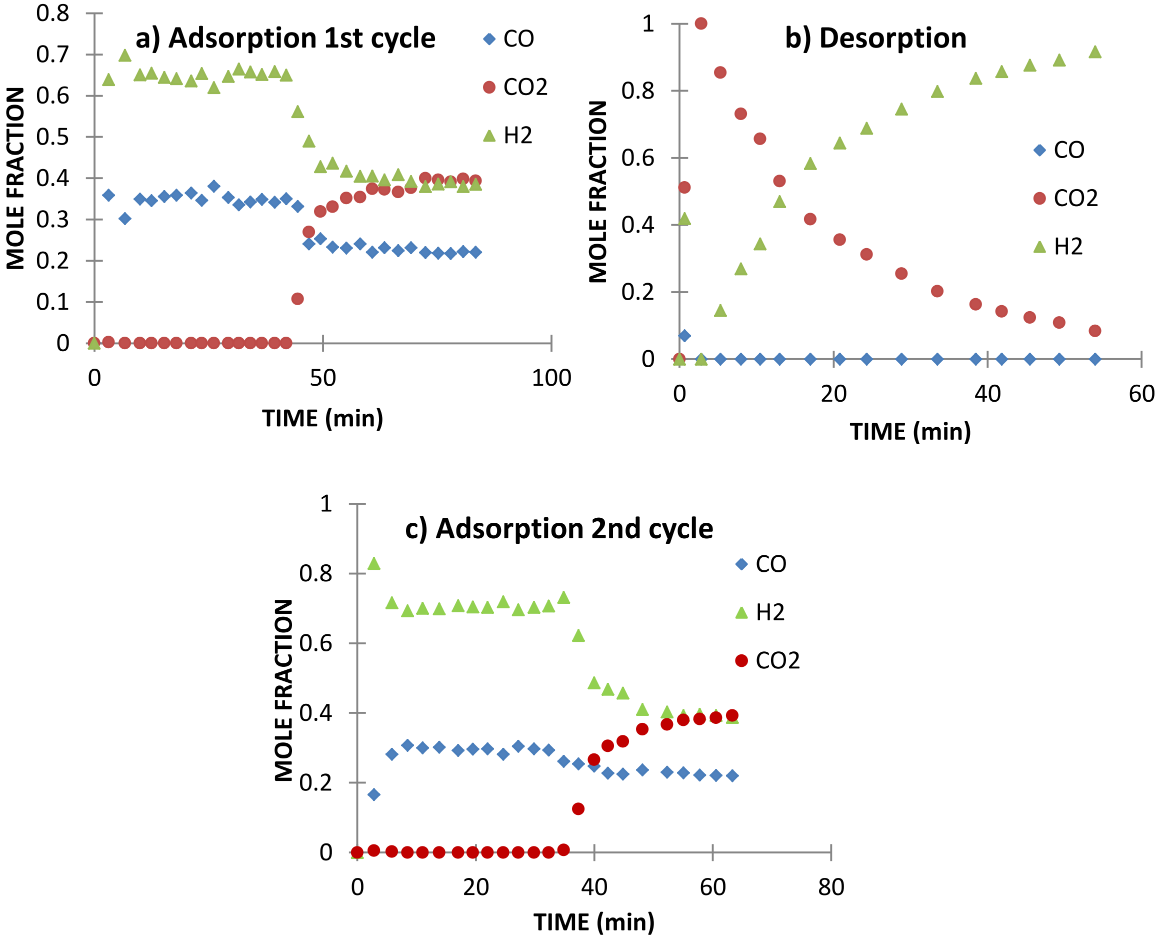

Figure 6: Breakthrough curves for adsorption/desorption: a) Adsorption on NaY for mixture of CO_2 (90 ml/min), CO (50ml/min) and H_2 (90 ml/min) at 295K and 1 atm. total pressure b) Desorption with H_2 at 373K and 30 ml/min c) Adsorption after desorption cycle with the same feed ad first cycle at 295K and 1 atm. total pressure.

As shown in Figure 6b, very small amount of CO was detected at the beginning during desorption. CO_2 was the only gas which being removed by H_2 at 373K during the entire blow down steps afterwards. Mole fraction of CO_2 in the outlet stream reached its maximum at 3 minutes and then decreased with time. Desorption of CO_2 was stopped after 54 minutes because of its very low flow rate (2.71 ml/min). Then adsorption separation of the mixture containing CO_2 (90 ml/min), CO (50 ml/min) and H_2 (90 ml/min) was started again in order to determine working capacity for the adsorbent. Table 3 shows the parameters of adsorption capacity and selectivity for first cycle and second cycle of adsorption (after desorption step).

Table 4: Comparison of adsorption capacity and selectivity factors for first cycle and second cycle adsorption.

Adsorbent	**Weight (g)**	**Cycle**	**Saturated water**	**Feed composition (ml/min) $CO_2/CO/H_2$**	**CO_2 Breakthrough (min)**	**CO Breakthrough (min)**	**CO_2 adsorption capacity (ml/g)**	**CO adsorption capacity (ml/g)**	**Selectivity**
NaY	64.91	1st	yes	90/50/90	42	-	66.43	2.1	17.41
NaY	65.81	2nd	yes	90/50/90	35	-	56.74	2.21	14.23

As shown in Table 4, zeolite NaY has shown CO_2 adsorption capacity of 56.74 ml/g which is more than 85% of the first cycle CO_2 adsorption capacity (66.43 ml/g) even though desorption temperature and purge gas flow rate were taken arbitrarily and have not been optimized yet. Also the time for blow-down step could be taken longer. This percentage is in agreement with adsorbent screening study in terms of expected working capacity at regeneration at elevated temperatures. Hence, zeolite NaY showed a promising working capacity for CO_2 adsorption. However more experiments should be carried out in order to determine stability of adsorbent for frequent adsorption/desorption cycles.

4.4. Summary and modeling parameters for different conditions

Figure 7 compares the empirical model and Rosen model used in this study with experimental results. As shown in this figure, the empirical model could be used for prediction of CO_2 breakthrough. Rosen model is slightly far from the experimental data; however the restrictions due to single component isothermal adsorption and mass transfer assumptions as well as ignoring the role of cation (in this case Na^+) in the zeolites could be reasons for this discrepancy. Therefore it is preferred to use empirical model with different parameters to predict breakthrough curves at different conditions.

Figure 8 presents a summary of all adsorption cycles with different circumstances in order to compare them in terms of CO_2 breakthrough and adsorption capacity. Table 4 presents adsorption capacity of the adsorbent and kinetic parameters of the adsorption in Yan model for each of the tested conditions.

Table 5: Modelling parameters for CO_2 adsorption at different conditions

Experiment	**Cycle**	**Water saturated**	**k_y (ml/min/g)**	**q_m (ml/g)**
1	**first**	**no**	**244.18**	**69.44**
2	**first**	**yes**	**224.34**	**62.92**
3	**second**	**yes**	**197.14**	**53.40**

As could be observed in Figure 8 and Table 5, CO_2 has the highest adsorption capacity at the first cycle with fresh adsorbent and as a dry gas without saturated water. Saturated stream passed through water can decrease breakthrough time compared to the dry stream since water molecules could compete with CO_2 adsorption. Although this effect could not be very significant in PSA industrial scale for CO_2/CO separation since water could be desorbed in regeneration cycle, it would be recommended to apply a desiccant bed to reduce relative humidity as low as possible prior to PSA system. Subsequently adsorption performance of a cycle after blow down step has been shown in Figure 8. As one would expect, the adsorption capacity was reduced due to some gases left in the adsorbent from desorption step. However it must be taken into account that blow down step was terminated after 54 minutes while there was still CO_2 coming out of the column. Hence, for a TSA application temperature could be increased or even it is possible to increase the rate of purge gas passing through the column in order to desorb more CO_2 in shorter cycle to increase the adsorption capacity in the next adsorption cycle. In the case of RWGS separation system, since H_2 eventually will be mixed with CO_2 at the inlet of the RWGS reactor, it would be profitable to pass H_2 stream with higher flow rate from PSA blow down columns and purge more CO_2 adsorbed in the adsorption bed instead of having an expensive vacuum system.

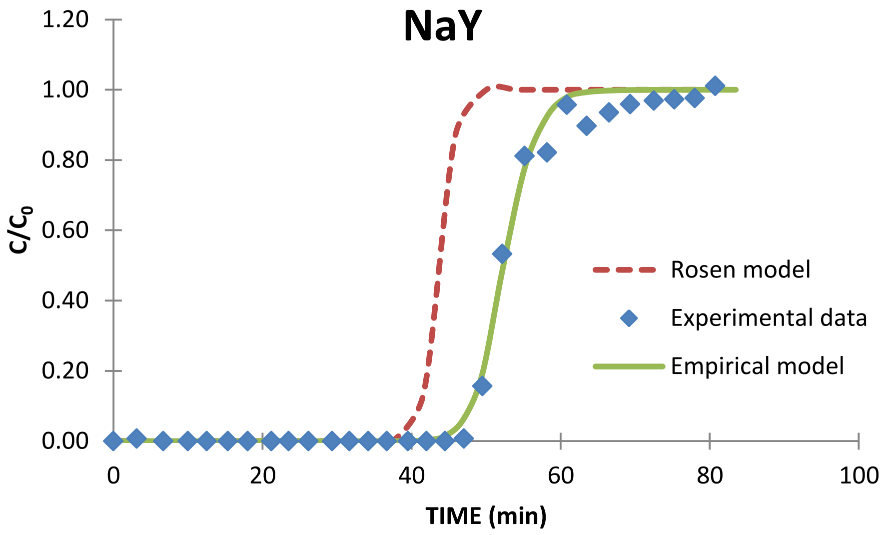

Figure 7: Comparison of Rosen model and empirical model for CO_2 adsorption by NaY at 1 atm and 294K.

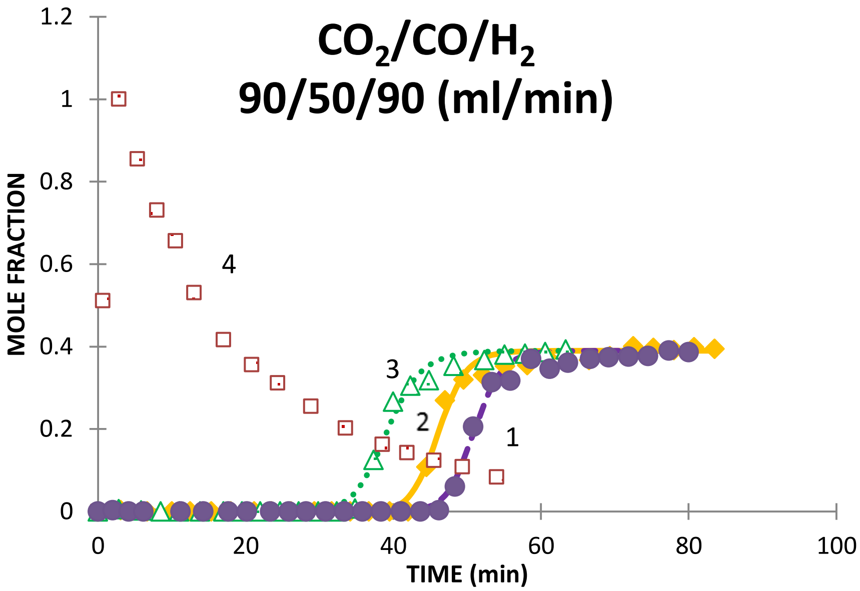

Figure 8: CO_2 outlet mole fraction in the multi component stream for different adsorption conditions at 313K:

1)● 1st cycle with dry stream (model: ------)
2)♦ 1st cycle with water saturated stream (model: ──)
3)Δ 2nd cycle after blow down with water saturated stream (model: ……..)
4)□ Blow down (CO_2 desorption)

5. Conclusions

Adsorption separation of CO_2/CO in a stream including CO_2/CO/H_2 saturated with water vapour was carried out successfully by zeolite NaY. CO_2 and CO could be easily separated under operating conditions of at 1 atm and ambient temperature in the presence of H_2 and saturated water. CO_2 broke through sooner for the saturated stream compared to the dry stream as expected, but it doesn't significantly affect the suitability of the adsorption process for the CO_2/CO separation. Empirical model was fitted better than Rosen model and its parameters were determined. Rosen model has some limited assumptions but more important is that this model cannot consider the effect of interaction between cation Na+ and components during adsorption. Economic analysis should be done to verify if a dehydration system is needed prior to PSA system for this application. It was observed that TSA at regeneration temperature of 373K or higher could be a promising method for desorption of CO_2 by purging H_2 so that expensive vacuum system won't be required. Also it would be recommended to do more adsorption desorption cycles in order to find stability of zeolite NaY and its life time at different desorption conditions. For this separation system downstream of RWGS reactor, it is possible to separate unreacted CO_2 and recycle it back to the reactor. Therefore CO_2 conversion to CO in the boundaries of the RWGS process would be maximized, resulting in producing more valuable CO for synthetic fuel production and mitigation of CO_2 emission as a GHG gas.

6. References

Abdollahi, F., F.H. Tezel, and S. Aplin, (2012). "Increasing conversion of CO_2 to CO via RWGS reaction: Simulation and process design", submitted to Alternative Energy.

Abdollahi, F., F.H. Tezel, and S. Aplin, (2013). "An experimental adsorbent screening study for separation of CO_2 from CO", to be submitted to Purification and Separation Technology Journal.

Cavenati, S., C. A. Grande and A. E. Rodrigues (2006). "Separation of $CH_4/CO_2/N_2$ mixtures by layered pressure swing adsorption for upgrade of natural gas." Chemical Engineering Science **61**(12): 3893-3906.

Grande, C. A. and A. E. Rodrigues (2008). "Electric swing adsorption for CO_2 removal from flue gases." International Journal of Greenhouse Gas Control **2**(2): 194-202.

Hashi, M., F. H. Tezel and J. Thibault (2010). "Ethanol recovery from fermentation broth via carbon dioxide stripping and adsorption." Energy & Fuels **24**: 4628-4637.

Walton, K. S. and M. D. LeVan (2006). "A novel adsorption cycle for CO_2 recovery: Experimental and theoretical investigations of a temperature swing compression process." Separation Science and Technology **41**(3): 485-500.

Yang, R. T. (1997). Gas separation by adsorption processes (Chapter3). London: Imperial College Press

Zhang, J., P. A. Webley and P. Xiao (2008). "Effect of process parameters on power requirements of vacuum swing adsorption technology for CO_2 capture from flue gas." Energy Conversion and Management **49**(2): 346-356.

Chapter V: Conclusion and Recommendations

Conclusions

Carbon capture and sequestration (CCS) plants in near future will provide significant amount of captured CO_2 which could be used as a raw material to produce low carbon liquid fuel through conventional processes such as the Fischer-Tropsch process. Conversion of CO_2 to CO as an active precursor for synthetic fuel production is important step of the process. The Reverse Water Gas Shift (RWGS) reaction, as the most suitable route to convert CO_2 to CO, has been studied in this thesis. A literature review and process simulation was conducted and the best operating conditions were evaluated. Based on overall CO_2 conversion and the factors which affect the process conversion, an integrated separation system downstream of the RWGS reactor has been suggested. By separating unreacted CO_2 and H_2 and recycling them back to the RWGS reactor, considering a conservative 80% recovery by the separation, the overall conversion of CO_2 to CO will be 75% which is higher than other suggested processes in the literature for the same operating conditions (temperature, pressure, and mole fraction). Also the energy consumption due to avoiding multistage reactors would be less.

Since gas separation by adsorption has been one of the most cost effective and efficient processes in the industrial scale, adsorbent screening experiments were performed in order to find the best adsorbent for CO_2/CO separation at the conditions downstream of the RWGS reactor. After literature review, four adsorbents were chosen as main candidates for comprehensive adsorbent screening. All results were fitted with the Langmuir and Toth Temperature-Dependent isotherms and Toth model worked better than Langmuir model; also important factors such as selectivity, adsorption capacity, the isosteric heat of adsorption, breakthrough curves and expected working capacity were determined. Finally zeolite NaY has shown to be the most promising adsorbent for CO_2/CO separation downstream of the RWGS reactor.

In order to validate the adsorbent screening tests and also obtaining adsorption design parameters, breakthrough experiments were carried out for real multicomponent mixtures based on the downstream composition and conditions of the RWGS reactor. The results were in very good agreement with the results of the adsorbent screening tests, for zeolite NaY as the best adsorbent in the operating conditions used. Separation of CO_2 from CO in the presence of H_2 and saturated by water showed very satisfactory performance and breakthrough curves were fitted by a modified empirical model, as well as the Rosen model. Empirical model was a better tool to simulate breakthrough curves since it has adjustable parameters compared to Rosen model. In order to test the working capacity of the adsorbent, blow down step (desorption) was conducted at elevated temperature of $100^{o}C$ with H_2 as the purge gas. Desorption of the CO_2 from the adsorbent showed validity of the adsorption test and expected working capacity. Also the main advantage was the successful desorption of CO_2 by H_2. As H_2 should be mixed with CO_2 at the inlet of RWGS reactor, it is not necessary to separate desorbed CO_2 from H_2 so that in industrial scale it reduces the cost of providing the inert gas for purging CO_2. On the other hand, the energy needed for elevating temperature for a TSA system would be provided from RWGS outlet since it needs to be cooled down prior to the condenser. Therefore a TSA system downstream of the RWGS reactor could successfully separate and recycle back un-reacted CO_2 to the rector with a recovery higher than 85% and would be a promising process for conversion of CO_2 to CO. Subsequently reduction of GHG emission and natural resource consumption are the main advantages of CO_2 to CO conversion in order to produce synthetic fuel in Canada.

Recommendations

The experiments conducted were carried out to characterize the adsorption separation of CO_2 and CO. More experiments are recommended for pilot plant RWGS reactor as well as the use of advanced simulation tools such as ADSIM in order to achieve less restricted modeling for the adsorption predictions. Also it would be very beneficial that separation experiments would be carried out in the lab scale for PSA or TSA in order to study the probability of deterioration of the adsorbents by repeated adsorption cycles and its stability in the industrial scale. A RWGS reactor catalyst study is recommended in order to identify an active and stable catalyst. For accomplishing the project and jump to a demonstration scale, it is also necessary to conduct an economic analysis for H_2 production from off-peak or renewable energy and its integration with RWGS process.